TECHNICAL NOTES

NATIONAL ADVISORY COMMITTEE FOR AERONAUTICS

No. 589

THEORETICAL SPAN LOADING AND MOMENTS OF TAPERED WINGS PRODUCED BY AILERON DEFLECTION

By H. A. Pearson
Langley Memorial Aeronautical Laboratory

Washington
January 1937

NATIONAL ADVISORY COMMITTEE FOR AERONAUTICS

TECHNICAL NOTE NO. 589

THEORETICAL SPAN LOADING AND MOMENTS OF TAPERED WINGS PRODUCED BY AILERON DEFLECTION

By H. A. Pearson

SUMMARY

The effect of tapered ailerons on linearly tapered wings is theoretically determined. Four different aileron spans are considered for each of three wing aspect ratios and each of four wing taper ratios. The change in lift on one half of the wing, the rolling moment, the additional induced drag, and the yawing moment, due to aileron deflection, are represented by nondimensional coefficients. Similar coefficients are given for the damping and yawing moments, the additional drag, and the change in lift, due to rolling.

It was found possible to effect a fairly close agreement between the theoretical and experimental rolling moments by introducing into the theoretical expression for the rolling moment an effective change in angle of attack obtained from an analysis of flap data. The theoretical curves show that the highly tapered wing with long ailerons has a lower ratio of yawing to rolling moment and a lower additional induced drag than wings with less taper.

INTRODUCTION

Airfoil theory may often be applied to the solution of practical aerodynamic problems. Even when the agreement between theory and experiment has not been good quantitatively, there has generally been a qualitative agreement and, for such cases, it is possible to determine correction factors by which the theory may be brought into agreement with experiment.

The theory has been applied (references 1 and 2) to determine the aerodynamic forces produced by aileron deflection and their distribution on rectangular wings of

various aspect ratios. Munk (reference 3) investigated the aileron effect on an elliptical wing of aspect ratio 6, and the computations have been extended (reference 2) to include aspect ratios of 3 and 9. Scarborough (reference 4) investigated in a general way the effect of twist such as might be caused by aileron deflection on both a rectangular and an elliptical wing.

The distribution of lift across the span is generally obtained by expressing the circulation as either a power or a Fourier series although it may be determined by a method of successive approximation. Probably the best known is the Fourier series solution, first used by Glauert and outlined in reference 5, in which the value of the lift is computed at four points across the semispan. In the case of an airfoil of irregular plan form or of one in which the section angle of attack changes abruptly, as when ailerons or flaps are operated, a larger number of points must be used to obtain an accurate distribution. The use of more points materially increases the labor as the number of simultaneous equations to be solved increases directly with the number of points.

Dr. Lotz (reference 6) has developed a slightly different method based on the Fourier solution by which the number of points may be increased with a less than proportional increase in labor, and which may readily be used on wings with complex plan forms and twists; however, the load distribution at the aileron end would not be sharply defined. This method is, nevertheless, adaptable to the general case and has been applied in several instances to compute the span load distribution of various odd types of wings.

Recently Lippisch (reference 7) developed another method for determining the spanwise distribution which is, like that of reference 6, applicable to the general case.

The method of successive approximation given in reference 8 and in a modified form in reference 9 has been little used partly because of its graphical nature and partly because of the time involved in obtaining a solution.

A method proposed by Gates (reference 10) combines a Fourier series and a least-squares solution. By the use of this method the general lift equation is satisfied at all points along the semispan while only a few harmonics

are retained; thus the shape of the span load distribution near the aileron end can be made definite. Hartshorn (reference 2) extended this method, which was originally used in determining the characteristics of a rectangular wing with tip elevators, to ailerons on rectangular and elliptical wings.

In the present report the computations have been extended to include the case of ailerons on linearly tapered wings of various aspect ratios. The method of Gates has been used in preference to the others, not because it is any more accurate, since all methods yield the same result if sufficient points are taken, but because definite numerical results are obtained with probably the least work. This statement holds for the case in which both the angle of attack and the chord distribution may be expressed as simple analytical functions.

LIFT AND ROLLING MOMENT DUE TO AILERONS

Lift at a section.- The coordinate y along the span b, in accordance with convention used in airfoil theory, is replaced by the parameter θ (fig. 1) so that

$$y = -\frac{b}{2}\cos\theta \tag{1}$$

The circulation at a section can be represented by the Fourier series

$$\Gamma = 2b\,V\,\Sigma\,A_n \sin n\theta \tag{2}$$

If the circulation Γ is symmetrical about the wing center line, i.e., if $\Gamma_\theta = \Gamma_{\pi-\theta}$, only odd values of n are retained. If the circulation is antisymmetrical, as would occur with equally and oppositely displaced ailerons on an airfoil giving no lift, only even values of n are needed. For the general case both the odd and the even values of n are required.

The induced velocity at a point can be given by the series

$$w = V\,\Sigma\,n\,A_n \frac{\sin n\theta}{\sin\theta} \tag{3}$$

The circulation Γ is also expressed by the relation

$$\Gamma = \frac{c_l cV}{2} = \frac{m_0 cV}{2}\left(\alpha - \frac{w}{V}\right) \qquad (4)$$

where c_l is the section lift coefficient

c, section chord

V, wind velocity

m_0, slope of section lift curve, per radian

α, section angle of attack, radians

w, downwash velocity

For linearly tapered wings the chord at any station is defined by the expression

$$c = c_r\,[1 \pm (1 - \lambda)\cos\theta] = c_r\,(1 \pm K\cos\theta) \qquad (5)$$

where c_r is the root chord

λ, ratio of tip to root chord

$K = (1 - \lambda)$

In equation (5) the minus sign is used to the left of the origin and the plus sign to the right. The general circulation equation for the linearly tapered wing,

$$\alpha u_0 (1 \pm K\cos\theta)\sin\theta = \sum A_n \sin n\theta\,[n u_0 (1 \pm K\cos\theta) + \sin\theta] \qquad (6)$$

where u_0 is a constant equal to $\frac{m_0 c_r}{4b}$, was obtained by introducing the values of Γ, w, and c as given by equations (2), (3), and (5), into equation (4) and by collecting the terms.

Figure 2 gives plots of values of u_0 for various taper ratios λ and aspect ratios A for $m_0 = 6$, instead of 2π, the theoretical value.

The change in wing section caused by an aileron deflection δ, in radians, may be considered equivalent to a change in geometric angle of attack of the section. This change may be denoted by $(k\delta)$ where k is a function of the aileron to wing chord ratio E. Now, according to the assumptions upon which wing theory is based, the distribution caused only by the ailerons may be superposed on the distribution of lift for ailerons neutral, since the lift distribution over the span is a linear function of the angle of attack at each point of the span. That the distributions may be superposed is indicated by an examination of equation (6), in which the right-hand summation can be divided into terms containing only odd coefficients, ailerons neutral; and terms containing even coefficients, ailerons deflected.

Only the even coefficients are retained at present; hence only the distribution due to aileron displacement will be found. Let the lift of the wing be zero and let $(k\delta)$ equal the increase or decrease of angle of attack of the section due to aileron displacement. Then $\bar{\alpha} = (k\delta)$ from $\theta = 0$ to $\theta = \varphi$ (fig. 1); 0 from $\theta = \varphi$ to $\theta = \pi - \varphi$; and $-(k\delta)$ from $\theta = \pi - \varphi$ to π. The inner ends of the ailerons are given by

$$y = -\frac{b}{2}\cos\varphi \quad \text{and} \quad y = -\frac{b}{2}\cos(\pi - \varphi) \qquad (7)$$

In the subsequent analysis the equations apply to cases in which: (1) E, the ratio of aileron to wing chord, is constant; (2) an equal up-and-down aileron movement occurs; (3) the wing tips are straight; and (4) the aileron extends inboard from the wing tip. The usual assumptions underlying modern wing theory are made. Although the foregoing limitations are made in this report, the method may be applied to cases where E is not constant provided that the change in angle of attack produced by such an aileron may be expressed as a simple function in terms of the parameter θ. A similar statement applies to the airfoil plan form, and the aileron need not extend

to the tip. A differential aileron motion may be considered as the sum of effects produced by a nondifferential aileron movement plus the effect produced by deflecting the ailerons as flaps.

The general circulation equation (6) can be represented by equations of the type

$$\Sigma A_n P_n = B \tag{8}$$

where $P_n = [n u_o (1 \pm K \cos \theta) + \sin \theta] \sin n\theta$ (9)

and $B = u_o \alpha (1 \pm K \cos \theta) \sin \theta$ (10)

The method proposed by Gates (reference 10) is based on the assumption that the conditions can be satisfied by retaining a small number of harmonics in the series provided that the general circulation equation is satisfied at an infinite number of points along the span. A number of equations of the form (8), where θ varies in infinitely small steps from 0 to π, is thus obtained. If only n harmonics are retained, a set of n simultaneous equations can be formed by the method of least squares and, in the limit, the summations are replaced by integrations. This method leads to n equations of the following type:

$$\left.\begin{aligned}
&A_2 \int_0^{\frac{\pi}{2}} P_2^2 \, d\theta + A_4 \int_0^{\frac{\pi}{2}} P_2 P_4 \, d\theta + \ldots A_{2n} \int_0^{\frac{\pi}{2}} P_2 P_{2n} \, d\theta = \int_0^{\frac{\pi}{2}} B P_2 \, d\theta \\
&A_2 \int_0^{\frac{\pi}{2}} P_4 P_2 \, d\theta + A_4 \int_0^{\frac{\pi}{2}} P_4^2 \, d\theta + \ldots A_{2n} \int_0^{\frac{\pi}{2}} P_4 P_{2n} \, d\theta = \int_0^{\frac{\pi}{2}} B P_4 \, d\theta \\
&\cdots\cdots\cdots\cdots\cdots\cdots\cdots\cdots\cdots\cdots\cdots\cdots\cdots\cdots\cdots\cdots \\
&A_2 \int_0^{\frac{\pi}{2}} P_{2n} P_2 \, d\theta + A_4 \int_0^{\frac{\pi}{2}} P_{2n} P_4 \, d\theta + \ldots A_{2n} \int_0^{\frac{\pi}{2}} P_{2n}^2 \, d\theta = \int_0^{\frac{\pi}{2}} B P_{2n} \, d\theta
\end{aligned}\right\} \tag{11}$$

The coefficients on the left-hand side, called "plan-form coefficients" since the angle of attack does not appear, involve integration of terms of the type

$$P_p P_r = (\sin p\theta \, [pu_o (1 - K \cos \theta)] + \sin p\theta \sin \theta) \times$$

$$(\sin r\theta \, [ru_o (1 - K \cos \theta)] + \sin r\theta \sin \theta) \tag{12}$$

It was found in applying this method that, for taper ratios from 1.0 to 0.25, the retention of four harmonics was sufficient to determine quite accurately the span load distribution. There is no object in carrying the calculations too far since the theoretical lift distribution may show considerable deviation from the actual distribution at the wing tips and aileron ends. Reference 11 shows that the contribution of A_8 to the lift of one aileron is only about 1 percent of the total unless the aileron span is less than 0.1 b. It is later shown that the total wing lift depends only upon A_1, that the rolling moment depends only upon A_2, and that the yawing moment depends primarily upon the first four coefficients of the series.

The integration of the plan-form coefficients, equation (12) when four harmonics are retained, is given in table I, first in the general form involving u_o and K and then in numerical form giving particular values to K and u_o depending upon taper and aspect ratio. In the bottom part of table I, m_o is assumed to be 6 instead of 2π.

The coefficients on the right-hand side of equation (11), called "angle coefficients," involve integrations of terms of the type

$$\int_0^{\frac{\pi}{2}} BP_p = \int_0^{\frac{\pi}{2}} u_o \alpha (1 - K \cos \theta) \sin \theta [p u_o (1 - K \cos \theta) + \sin \theta] \sin p\theta \, d\theta \qquad (13)$$

and by the previous simplification this expression becomes

$$\int_0^{\frac{\pi}{2}} BP_p = \int_0^{\varphi} u_o(k\delta) (1 - K \cos \theta) \sin \theta [p u_o (1-K \cos \theta) + \sin \theta] \sin p\theta \, d\theta \qquad (14)$$

Thus the point along the span at which the aileron starts is definitely fixed by the upper limit of the integral equation (14). The integration for the angle coefficients is given in general and numerical form in table II for four different aileron span ratios, b'/b. The reason for retaining $u_o(k\delta)$ in the denominator will be seen later.

The first four terms of the circulation series for

the even coefficients, in terms of the angle coefficients, are given in table III. These coefficients are obtained by solving the 12 sets of four simultaneous equations, as given by equation (11), regarding $\int_0^{\frac{\pi}{2}} BP_p$ as a new coefficient B_p.

The lift coefficients at a section due to aileron deflection is related to the circulation* (equations (2) and (4)) by

$$\frac{c_{l_a}}{2} cV = \Gamma = 2b V \Sigma A_{n_2} \sin n\theta \qquad (15)$$

Substituting equation (5) for the chord

$$c_{l_a} = \frac{4b}{cr (1 \pm K \cos \theta)} \Sigma A_{n_2} \sin n\theta \qquad (16)$$

but $\frac{m_o c_r}{4b} = u_o$; hence $\frac{4b}{cr} = \frac{m_o}{u_o}$

so that $$c_{l_a} = \frac{m_o(k\delta)}{1 \pm K \cos \theta} \Sigma \frac{A_{n_2}}{u_o(k\delta)} \sin n\theta \qquad (17)$$

Similarly, the lift coefficient at a point with ailerons neutral is given by

$$c_{l_1} = \frac{m_o \alpha}{1 \pm K \cos \theta} \Sigma \frac{A_{n_1}}{u_o \alpha} \sin n\theta \qquad (18)$$

The total c_l at a section is the sum of the lift coefficients given by equations (17) and (18). The form of equation (17) indicates that the change in c_{l_a} due to aileron deflection is directly proportional to the equivalent change in angle of attack and that it is also a function of $\frac{A_{n_2}}{u_o(k\delta)}$. Values of $\frac{A_{n_2}}{u_o(k\delta)}$ are given in table IV for the various aspect ratios and taper ratios previously used and for four aileron lengths. The distribution of c_{l_a} due to aileron deflection is found by substituting the results from table IV in equation (17). This distri-

*Hereafter for even coefficients the subscript a will be used; for odd coefficients the subscript 1, and for both types no subscript.

bution is given in figure 3 for a value of $(k\delta)$ equal to 1.0. For any other value of $(k\delta)$ the ordinates of this figure need only be multiplied by the actual value of $(k\delta)$. In an actual case the effective change in angle of attack at a section can be theoretically computed (reference 11) or, preferably, can be obtained from an analysis of flap data such as that given in reference 12. At fairly large values of δ the experimental value of k hardly ever exceeds 0.2 and would equal 1.0 only if a whole wing section, such as one with floating wing-tip ailerons, were deflected.

The lift distribution due to the ailerons obtained from figure 3 must be superposed on the c_{l_1} distribution due to angle of attack of the wing as a whole (equation (18)) to obtain the total distribution. The c_{l_1} distribution and the A_{n_1} coefficients corresponding to a wing C_L of 1.0 are given in figure 4 and table V, respectively. These values, taken from an unpublished report, have been determined by the Lotz method using 10 points across the semispan and retaining 4 harmonics. The c_{l_1} distribution and A_{n_1} coefficients at any other value of the wing C_L are obtained by multiplying by the new value of the wing C_L. Figure 5 illustrates the procedure used to find the span c_l distribution under the following conditions:

$$\lambda, \quad 0.5$$

$$\frac{b'}{b}, \quad 0.6$$

$$(k\delta), \quad 0.10$$

$$C_L, \quad 0.65$$

$$A, \quad 6$$

Change in lift on half the wing.- The change in lift on one half of the wing is given by

$$\Delta \text{ lift} = \int_0^{\frac{b}{2}} c_{l_2} \, qc \, dy \qquad (19)$$

Substituting the values of c_{l_2} and c from equations

(17) and (5) and $\frac{b}{2} \sin \theta \, d\theta$ for dy

$$\Delta \text{ lift} = qm_o(k\delta) \, c_r \frac{b}{2} \int_0^{\frac{\pi}{2}} \Sigma \frac{A_{n_2}}{u_o(k\delta)} \sin n\theta \sin \theta \, d\theta \quad (20)$$

Integrating

$$\Delta \text{ lift} = qm_o(k\delta) \, c_r \frac{b}{2} F_1 = 2qb^2 (k\delta) F_1 \quad (21)$$

where

$$F_1 = u_o \Sigma (-1)^{\frac{n_2+2}{2}} \frac{n_2}{n_2^2 - 1} \frac{A_{n_2}}{u_o(k\delta)}$$

Values of F_1 are tabulated in table VI and are plotted in figure 6 for various wing aspect ratios and taper ratios.

Total lift.- The total lift on the wing is given by

$$\text{Lift} = \int_{-\frac{b}{2}}^{\frac{b}{2}} c_{l_1} cq \, dy \quad (22)$$

where c_{l_1} is that for a neutral position of the aileron.

Substituting for c_{l_1}, c, and dy, the foregoing expression becomes

$$\text{Lift} = 2qb^2 \int_0^{\pi} \Sigma A_{n_1} \sin n\theta \sin \theta \, d\theta \quad (23)$$

Integrating

$$\text{Lift} = \pi q b^2 A_1 \quad (24)$$

Thus the total lift depends upon only the first term of the series.

Rolling moment.- The rolling moment for the semispan is determined from the expression

$$\frac{L}{2} = \int_0^{\frac{b}{2}} c_{l_2} cqy \, dy \quad (25)$$

Substituting for c_{l_2}, c, y, and dy in (25), the values given by equations (17), (5), and (1)

$$\frac{L}{2} = \frac{qm_o(k\delta)\ c_r\ b^2}{8} \int_0^{\frac{\pi}{2}} \Sigma\ \frac{A_n}{u_o(k\delta)} \sin n\theta\ \sin 2\theta\ d\theta \qquad (26)$$

The value of the integral is always zero when the lower limit is substituted, but only one value of n, namely, 2, gives the integral a value when the upper limit is substituted. This value is $\pi/4$, hence

$$\frac{L}{2} = \frac{qm_o(k\delta)\ c_r\ b^2}{8} \frac{\pi\ A_2}{4u_o(k\delta)} = qb^3(k\delta)\ F_2 \qquad (27)$$

where

$$F_2 = \frac{\pi u_o}{8} \left(\frac{A}{u_o(k\delta)}\right)$$

The lateral center of pressure of the change in load due to aileron displacement is

$$c.p. = \frac{\frac{L}{2}}{\Delta\ lift} = \frac{F_2}{F_1}\ \frac{b}{2} \qquad (28)$$

Values of F_2 are tabulated in table VII and plotted in figure 7; the ratio of F_2/F_1 is plotted in figure 8.

INDUCED DRAG AND YAWING MOMENT DUE TO AILERONS

Induced drag at a section.- The induced drag coefficient at a section is given by

$$c_{d_i} = c_l\ \frac{w}{V} \qquad (29)$$

and substituting for w and c_l the values given by equations (3) and (16) with both odd and even coefficients

$$c_{d_i} = \frac{4b}{c_r(1 \pm K \cos\theta) \sin\theta} \Sigma A_n \sin n\theta\ \Sigma n A_n \sin n\theta \qquad (30)$$

If a total of 8 harmonics are retained i.e., 4 odd and 4 even, a large number of terms resulting from expanding the foregoing equations may be divided into three groups; the first group is composed of terms in which combinations of odd terms are multiplied together; the second group, of terms in which combinations of even terms are multiplied; and the third group, of all combinations of even and odd coefficients. If the ailerons were neutral and the wing were lifting, only terms of the first group would appear. With displaced ailerons and the wing at zero lift, only terms of the second group would occur. The terms of the third group can then be said to arise from the interaction of the neutral distribution and the distribution due to the ailerons.

Induced drag for the wing.- The total induced drag for the wing is given by

$$D_i = \int_{-\frac{b}{2}}^{\frac{b}{2}} c_{d_i}\, qc\,dy \qquad (31)$$

After values of c_{d_i}, c, and dy are substituted

$$D_i = 2qb^2 \int_0^{\pi} \Sigma A_n \sin n\theta \; \Sigma n A_n \sin n\theta \; d\theta \qquad (32)$$

Performing the multiplications indicated under the summation signs, terms of the type $\sin^2 n\theta$ and $\sin p\theta \sin r\theta$ result. The lower limit of this integral is always zero. Only terms of the type $nA_n^2 \sin^2 n\theta$ give values to the integral for the upper limit; hence (32) becomes after integrating

$$D_i = \pi q b^2 \Sigma n A_n^2 \qquad (33)$$

This latter expression can be divided into two parts

$$D_i = \pi q b^2 \Sigma n_1 A_{n_1}^2 + \pi q b^2 \Sigma n_2 A_{n_2}^2 \qquad (34)$$

in which the first part represents the ordinary induced drag and the second part, the additional induced drag due to aileron displacement. The first part, rearranged, can be written as

$$D_i = \frac{C_L^2\, qS}{\pi A}(1 + \sigma) \qquad (35)$$

the well-known formula for induced drag in which $(1 + \sigma)$ is equal to $\Sigma \frac{n_1 A_{n_1}^2}{A_1^2}$. Values of σ obtained from reference 5 are shown in figure 9 for an aspect ratio of 6. The formula for the total induced drag becomes

$$D_i = \frac{C_L^2 \, qS}{\pi A} (1 + \sigma) + \pi q b^2 F_3 (k\delta)^2 \qquad (36)$$

where $$F_3 = \Sigma n_2 A_{n_2}^2.$$

Table VIII and figure 10 give values of F_3 for $(k\delta)$ equal to 1.0 at the various wing aspect ratios and taper ratios previously used. The magnitude of F_3 for other values of $(k\delta)$ is determined by multiplying the given F_3 factors by the square of the actual value of $(k\delta)$.

Although the previous section showed that the distribution of induced drag could be separated into three component parts, equation (34) shows that the resultant of the distribution due to the interaction effect must be zero.

Yawing moment.- When the ailerons are displaced the lift is increased on one side of the wing and decreased on the other so that the induced-drag distribution is modified. Thus, in addition to the desired rolling moment, a yawing moment arises because of the unsymmetrical distribution of the induced drag. This yawing moment is given by

$$N = \int_{-\frac{b}{2}}^{\frac{b}{2}} c_{d_i} \, cqy \, dy \qquad (37)$$

Substituting for c_{d_i}, c, y, and dy

$$N = qb^3 \int_0^{\pi} \Sigma n A_n \sin n\theta \; \Sigma A_n \sin n\theta \cos\theta \, d\theta \qquad (38)$$

Performing the indicated multiplications and integrating between the limits 0 and π for eight harmonics

$$N = \frac{\pi q b^3}{4} (3A_1A_2 + 5A_2A_3 + 7A_3A_4 + 9A_4A_5 + 11A_5A_6 + 13A_6A_7 + 15A_7A_8) \qquad (39)$$

Now the rolling moment for the entire wing can be written as

$$L = \frac{\pi q b^3}{4} A_2 \qquad (40)$$

so that the ratio of the yawing to the rolling moment is

$$\frac{N}{L} = 3A_1 + 5A_3 + 7A_5 \frac{A_4}{A_2} + 9A_5 \frac{A_4}{A_2} + 11A_5 \frac{A_6}{A_2} + 13A_7 \frac{A_6}{A_2} + 15A_7 \frac{A_8}{A_2} \qquad (41)$$

This ratio, which is independent of aileron deflection and dependent only on the lift and wing plan form, is plotted in figure 11 and tabulated in table IX for a total wing C_L of 1.0. In order to obtain the ratio at any other value of wing C_L, multiply the results of figure 11 by the C_L for which N/L is desired. Munk (reference 13) has determined an expression for the elliptical wing similar to equation (41).

FACTORS FOR THE ROLL

The previously derived coefficients and factors are those effective when the ailerons are first deflected. As the wing begins to rotate, a damping moment proportional to the angular velocity is introduced. The changes produced by the roll may also be considered separately and may be superposed on the initial conditions. The effect of the roll is quite similar to the effect due to ailerons with equal and opposite deflection since the resulting load distribution is antisymmetrical. The change in angle of attack varies along the span and is given by

$$\Delta\alpha = \frac{p'y}{V} = -\frac{p'b \cos\theta}{2V} \qquad (42)$$

where p' is the angular velocity in roll with respect to the wind axis.

Equations (1) to (13) also apply to the roll. Substituting in (13) the value of $\Delta\alpha$ given by (42)

$$\int_0^{\frac{\pi}{2}} BP_p = \int_0^{\frac{\pi}{2}} \left[u_o \left(\frac{p'b}{2V}\right) \cos\theta \sin\theta (1 - K\cos\theta)\right] \left\{\sin p\theta \left[pu_o (1 - K\cos\theta) + \sin\theta\right]\right\} d\theta \qquad (43)$$

which can be integrated regarding u_o and $\left(\frac{p'b}{2V}\right)$ as constants.

The lift at a section due to rolling is given by an equation analogous to (17)

$$c_{l_2} = \frac{m_o \left(\frac{p'b}{2V}\right)}{1 \pm K \cos \theta} \Sigma \frac{A_{n_2}}{u_o \left(\frac{p'b}{2V}\right)} \sin n\theta \qquad (44)$$

Values of $\frac{B_p}{u_o \left(\frac{p'b}{2V}\right)}$ and $\frac{A_{n_2}}{u_o \left(\frac{p'b}{2V}\right)}$ are given in table X for the different taper ratios and aspect ratios previously used. The following equations are derived by the previous method.

The increase in lift on half the wing

$$\Delta \text{ lift} = q m_o \left(\frac{p'b}{2V}\right) c_r \frac{b}{2} F_4 = 2qb^2 \left(\frac{p'b}{2V}\right) F_4 \qquad (45)$$

where $$F_4 = u_o \Sigma(-1)^{\frac{n_2+2}{2}} \frac{n_2}{n_2^2 - 1} \frac{A_{n_2}}{u_o \left(\frac{p'b}{2V}\right)}$$

Table XI and figure 12 give values of F_4.

The damping moment for the semispan is

$$\frac{L_D}{2} = \frac{q m_o \left(\frac{p'b}{2V}\right) c_r b^2}{8} \frac{\pi}{4} \frac{A_2}{u_o \left(\frac{p'b}{2V}\right)} = qb^3 \left(\frac{p'b}{2V}\right) F_5 \qquad (46)$$

where $$F_5 = \frac{\pi u_o}{8} \left(\frac{A_2}{u_o \left(\frac{p'b}{2V}\right)} \right)$$

Values of F_5 are given in figure 13 and in table XI. The total damping moment L_D is twice that given by (46).

The lateral center of pressure of the load due to rolling is given by $\frac{F_5}{F_4}\frac{b}{2}$.

Equations for the drag are similar to those of the preceding sections. The additional induced drag due to rolling is given by

$$D_i = \pi q b^6 F_6 \tag{47}$$

where $F_6 = \Sigma n_3 A_{n_3}^2$. The factor F_6 is plotted in figure 14 and tabulated in table XI for a value of $\frac{p'b}{2V}$ equal to 1.0.

Although in the determination of the damping moment it was possible to assume with little error that the effect of the roll could be replaced by a twisting of the wing, this assumption cannot be made in the determination of the yawing moment. This condition arises because the lift vectors, being perpendicular to the relative wind, are inclined with respect to an axis normal to the flight path and thus have components that tend to make the falling wing advance. The component of the induced drag tends to reduce this tendency as may be seen from figure 15, which shows the resolution of the lift and drag at a point y on the span when the air is rising to meet the wing.

The yawing moment due to the damping moment is given by

$$N_D = \int_{-\frac{b}{2}}^{\frac{b}{2}} c_l \sin\frac{yp'}{V} cqydy - \int_{-\frac{b}{2}}^{\frac{b}{2}} c_{d_i} \cos\frac{yp'}{V} cqydy \tag{48}$$

where $\sin\frac{yp'}{V}$ and $\cos\frac{yp'}{V}$ may be replaced by $\frac{yp'}{V}$ and 1.0, respectively. With this simplification equation (48) becomes

$$N_D = \frac{qp'}{V}\int_{-\frac{b}{2}}^{\frac{b}{2}} c_l cy^2 dy - q\int_{-\frac{b}{2}}^{\frac{b}{2}} c_{d_i} cydy \tag{49}$$

After substituting for c_l, c, etc., and determining the value of the integral between the limits given

$$\frac{N_D}{q} = \frac{\pi b^3}{4}\left[\left(\frac{p'b}{4V}A_1 + \frac{p'b}{4V}A_3\right) - (3A_1A_2 + 5A_2A_3 + 7A_3A_4 + \right.$$

$$\left. + 9A_4A_5 + 11A_5A_6 + 13A_6A_7 + 15A_7A_8)\right] \quad (50)$$

Now the damping moment L_D can be written as

$$\frac{L_D}{q} = \frac{\pi b^3}{4}A_2$$

and hence the ratio of the yawing to the damping moment is

$$\frac{N_D}{L_D} = \frac{p'b}{4V}\left(\frac{A_1 + A_3}{A_2}\right) - \left(3A_1 + 5A_3 + 7\frac{A_3A_4}{A_2} + 9\frac{A_4A_5}{A_2} + \right.$$

$$\left. + 11\frac{A_5A_6}{A_2} + 13\frac{A_6A_7}{A_2} + 15\frac{A_7A_8}{A_2}\right) \quad (51)$$

This ratio is plotted in figure 16 and is tabulated in table XI for a total wing C_L of 1.0. The direction of the yawing moment is such as to make the falling wing move forward.

Equating (27) and (46) and solving for $\frac{p'b}{2V}$ gives the maximum obtainable theoretical value of this ratio as

$$\left(\frac{p'b}{2V}\right)_{max} = \frac{F_2}{F_5}(k\delta) \quad (52)$$

Average values of F_2/F_5 are shown by the solid curve plotted in figure 17. The maximum deviations from the average due to changes in aspect ratio and taper are of minor importance as shown by the narrowness of the envelope lines.

DISCUSSION

The span c_{l_2} distribution curves of figure 3 indicate that the additional load on half the wing, at equal values of $(k\delta)$, increases with aspect ratio and aileron span; figure 6 shows that it decreases with increase in taper (i.e., λ decreases). The distribution curves of figures 3 and 4 indicate that as the taper increases the points of maximum c_{l_1} and c_{l_2} move outward. This type

of variation arises because the inboard sections, which give the greater lift, induce an additional lift on the weaker outboard sections, resulting in an increase of c_l toward the tip on the tapered wings. This increase, which becomes greater with increasing taper, introduces no theoretical difficulties, but in practice a condition is reached in which the tip sections would stall before the rest of the airfoil. Figure 18, which gives the results of tests (reference 14) made of a series of untwisted wings, is included as an illustration; the point that stalls first moves outward as the taper increases. Although not indicated by figure 18, a comparison between the original experimental and the theoretical c_{l_1} curves of the pointed wing indicates that the tip sections of such a wing actually begin to stall at very low wing lift coefficients.

As will be mentioned in more detail later, the tendency of sharply tapered wings to stall first at the tip introduces problems of considerable importance in lateral control and stability near the stall. In general, it may be said that a sharply tapered wing, to be satisfactory from this standpoint, should be designed in such a way as to prevent premature stalling of the tips. This result can be accomplished, presumably, by any of several expedients, including washing out the wing or using slots or similar devices. Whether the sharply tapered wing, using such devices, is superior to plain wings with less taper, is a question outside the scope of this paper.

The theoretical rolling-moment factors (fig. 7) indicate that the available rolling couple, for equal values of $(k\delta)$, increases with both aileron span and λ, while equation (27) shows that the couple also increases with wing span. Short ailerons on highly tapered wings would give a rolling moment of about one-half that of a rectangular wing of similar aspect ratio and span when compared at equal values of $(k\delta)$. This variation arises principally because the area immediately affected by the aileron would be less for the tapered wing. For ailerons covering 0.8b the ratios of the moments are considerably increased and it is apparent that, if the lateral moments of inertia were taken into account, the highly tapered wing would be superior to the rectangular wing for control below the stall. It should be pointed out, however, that the tendency of the tips of sharply tapered wings to stall first will result in reduced lateral control with ordinary ai-

lerons at angles of attack near the stall. The theoretical superiority of the tapered wing with long-span ailerons may not, therefore, be completely realized in practice.

References 15 and 16 give the results of tests of a series of rectangular and tapered wings with rectangular and tapered ailerons with which the theoretical values of this report are compared in figure 19 for three taper ratios. The rolling-moment coefficients tabulated in references 15 and 16 are related to the F_2 factor of this report by

$$C_l' = 2A\,(k\delta)\,F_2$$

The effective values of $(k\delta)$ for the comparison have been obtained from reference 12 by considering the lift increments given there for the full-span flap as equivalent to $m(k\delta)$ where m, the slope of the lift curve, has a value of 4.35 per radian. (This value corresponds to an average value for a wing of aspect ratio 6.) Since the value of $(k\delta)$ so obtained is for a down aileron, only those cases (references 15 and 16) in which one aileron was down and the other was neutral were used in the comparison. Wherever possible the comparison has been made for values of δ of 10°, 20°, 25°, 30°, and 35° and for wing angles of attack of 0°, 10°, and 14°. In the case of the wings with λ equal to 1.0 and 0.6, the agreement is fair but, for the wing with λ equal to 0.2, the computed values are generally too high.

The lateral center-of-pressure curves for the additional load (fig. 8) indicate that the principal effect is due to the aileron span while aspect ratio and taper have only a minor influence.

The additional induced drag at equal values of $(k\delta)$ (fig. 10) increases directly with both b'/b and λ and inversely with aspect ratio. With short ailerons the tapered wing ($\lambda = 0.25$) would give an additional drag only half as large as the rectangular wing of equal area and aspect ratio; whereas, with long ailerons, the difference decreases as did the rolling-moment factor.

Figure 11 indicates that the ratio of yawing moment to the rolling moment at equal values of wing C_L decreases with an increase in wing taper, aileron span, or wing aspect ratio. Experiments (references 15 and 16)

confirm the theory that the ratio of yawing to rolling moment decreases with increase in taper below the stall. At or just above the stall, experiments (reference 15) indicate that the ratio increases with increasing wing taper until the yawing moments become so large that they cannot be controlled by the average rudder. This type of variation is a further result of the fact that the section which stalls first moves outward with increase in taper.

The factors due to an angular velocity (figs. 12 to 15, table XI) vary as do those arising from an aileron deflection. Although, theoretically, taper and aspect ratio have only a very minor influence on the maximum angular velocity attainable (fig. 17), the tapered wing will accelerate to this value sooner because of the lower inertia. The maximum value of $p'b/2V$ likely to be obtained in controlled flight in gusty air is 0.05, according to reference 16. This value corresponds approximately to the value that would be obtained with ailerons which are 0.15 of the wing chord, cover one-third of the span, and are deflected 15°.

SUMMARY OF THEORETICAL EQUATIONS

The characteristics of a wing with equally and oppositely deflected ailerons under static conditions may be given by the following equations:

Change in lift on half the wing, $\Delta L = 2qb^2(k\delta)\ F_1$ (fig. 6)

Total rolling moment, $L = 2qb^3(k\delta)\ F_2$ (fig. 7)

Additional induced drag $= \pi qb^2(k\delta)^2\ F_3$ (fig. 10)

Ratio of yawing to rolling moment, $\frac{\bar{N}}{L} = \left(\frac{\bar{N}}{L}\right)_{C_L=1.0} C_L$ (fig. 11)

The following equations refer to the wing in roll:

Change in lift on half the wing, $\Delta L = 2qb^2\left(\frac{p'b}{2V}\right) F_4$ (fig. 12)

Total damping moment, $L_D = 2qb^3\left(\frac{p'b}{2V}\right) F_5$ (fig. 13)

Additional induced drag $= \pi q b^2 \left(\frac{p'b}{2V}\right)^2 F_6$ (fig. 14)

Ratio of yawing to damping moment, $\frac{N}{L_D} = \left(\frac{N}{L_D}\right)_{C_L=1.0} C_L$ (fig. 16)

Maximum possible value of $\left(\frac{p'b}{2V}\right)$, $\left(\frac{p'b}{2V}\right)_{max} = \frac{F_2}{F_5}$ (kδ) (fig. 17)

Langley Memorial Aeronautical Laboratory,
National Advisory Committee for Aeronautics,
Langley Field, Va., November 16, 1935.

REFERENCES

1. Wieselsberger, C., and Asano, T.: Determination of the Air Forces and Moments Produced by the Ailerons of an Airplane. T.M. No. 488, N.A.C.A., 1928.

2. Hartshorn, A. S.: Theoretical Relationship for a Wing with Unbalanced Ailerons. R. & M. No. 1259, British A.R.C., 1929.

3. Munk, Max M.: On the Distribution of Lift Along the Span of an Airfoil with Displaced Ailerons. T.N. No. 195, N.A.C.A., 1924.

4. Scarborough, James B.: Some Problems on the Lift and Rolling Moment of Airplane Wings. T.R. No. 200, N.A.C.A., 1925.

5. Glauert, H.: The Elements of Aerofoil and Airscrew Theory. Cambridge University Press, 1926.

6. Lotz, Irmgard: Berechnung der Auftriebsverteilung beliebig geformter Flügel. Z.F.M., 22. Jahrgang 7. Heft 14. April 1931, S. 189-195.

7. Lippisch, A.: Method for the Determination of the Spanwise Lift Distribution. T.M. No. 778, N.A.C.A., 1935.

8. Fage, A.: On the Theory of Tapered Aerofoils. R. & M. No. 806, British A.R.C., 1923.

9. Jacobs, Eastman N., and Sherman, Albert: Wing Characteristics as Affected by Protuberances of Short Span. T.R. No. 449, N.A.C.A., 1933.

10. Gates, S. B.: An Analysis of a Rectangular Monoplane with Hinged Tips. R. & M. No. 1175, British A.R.C., 1928.

11. Glauert, H.: Theoretical Relationships for an Aerofoil with Hinged Flap. R. & M. No. 1095, British A.R.C., 1927.

12. Pearson, H. A.: A Method of Estimating the Aerodynamic Effects of Ordinary and Split Flaps on Airfoils Similar to the Clark Y. T.N. No. 571, N.A.C.A., 1936.

13. Munk, Max M.: A New Relation Between the Induced Yawing Moment and the Rolling Moment of an Airfoil in Straight Motion. T.R. No. 197, N.A.C.A., 1924.

14. Norton, F. H., and Bacon, D. L.: Pressure Distribution Over Thick Aerofoils - Model Tests. T.R. No. 150, N.A.C.A., 1922.

15. Weick, Fred E., and Wenzinger, Carl J.: Wind-Tunnel Research Comparing Lateral Control Devices, Particularly at High Angles of Attack. IX. Tapered Wings with Ordinary Ailerons. T.N. No. 449, N.A.C.A., 1933.

16. Weick, Fred E., and Wenzinger, Carl J.: Wind-Tunnel Research Comparing Lateral Control Devices, Particularly at High Angles of Attack. I - Ordinary Ailerons on Rectangular Wings. T.R. No. 419, N.A.C.A., 1932.

TABLE I

Values of $R_{pr} = \int_0^{\frac{\pi}{a}} P_p P_r \, d\theta$

$$= \int_0^{\frac{\pi}{a}} \left\{ \sin p\theta \left[pu_0(1 - K \cos\theta) \right] + \sin\theta \sin p\theta \right\} \left\{ \sin r\theta \left[ru_0(1 - K \cos\theta) \right] + \sin\theta \sin r\theta \right\}$$

Quantity	Value
R_{22}	$(\pi - 4.267\,K + \frac{\pi}{2}K^2)\,u_0^2 + (2.134 - 1.333\,K)\,u_0 + \frac{\pi}{8}$
R_{24}	$(-2.438\,K + \frac{\pi}{2}K^2)\,u_0^2 - 0.914\,u_0 - \frac{\pi}{16}$
R_{26}	$0.611\,K\,u_0^2 - (0.203 - 0.534\,K)\,u_0$
R_{28}	$-0.298\,K\,u_0^2 - 0.092\,u_0$
R_{44}	$(4\pi - 16.253\,K + 2\pi K^2)\,u_0^2 + (4.063 - 2.133\,K)\,u_0 + \frac{\pi}{8}$
R_{46}	$(-7.757\,K + \frac{3}{2}\pi K^2)\,u_0^2 - 1.616\,u_0 - \frac{\pi}{16}$
R_{48}	$1.910\,K\,u_0^2 - (0.359 - 0.914\,K)\,u_0$
R_{66}	$(9\pi - 36.252\,K + \frac{9}{2}\pi K^2)\,u_0^2 + (6.042 - 3.0864\,K)\,u_0 + \frac{\pi}{8}$
R_{68}	$(-15.749\,K + 3\pi K^2)\,u_0^2 - 2.297\,u_0 - \frac{\pi}{16}$
R_{88}	$(16\pi - 64.250\,K + 8\pi K^2)\,u_0^2 + (8.032 - 4.064\,K)\,u_0 + \frac{\pi}{8}$

Quantity \ λ	1.00			0.75			0.50			0.25		
A	4	6	8	4	6	8	4	6	8	4	6	8
R_{22}	1.635	1.119	0.903	1.565	1.086	0.878	1.477	1.037	0.847	1.370	0.977	0.807
R_{24}	-.539	-.424	-.368	-.683	-.500	-.415	-.860	-.592	-.477	-1.085	-.712	-.556
R_{26}	-.076	-.051	-.038	-.002	-.007	-.008	.108	.055	.035	.284	.152	.101
R_{28}	-.035	-.023	-.017	-.053	-.032	-.023	-.083	-.047	-.032	-.136	-.072	-.048
R_{44}	3.683	2.184	1.597	3.545	2.130	1.556	3.394	2.057	1.518	3.279	1.998	1.484
R_{46}	-.802	-.599	-.499	-1.193	-.793	-.618	-1.680	-1.034	-.769	-2.306	-1.346	-.966
R_{48}	-.135	-.089	-.067	.032	.002	-.006	.288	.139	.084	.712	.358	.227
R_{66}	6.634	3.650	2.521	6.353	3.544	2.441	6.063	3.408	2.373	5.883	3.319	2.324
R_{68}	-1.058	-.768	-.627	-1.798	-1.127	-.841	-2.725	-1.573	-1.116	-3.918	-2.149	-1.471
R_{88}	10.472	5.509	3.668	9.989	5.326	3.533	9.499	5.099	3.419	9.221	4.963	3.347

TABLE II

Values of $B_p = \int_0^{\pi} BF_p \, d\theta$

$= u_o(k\delta) \int_0^{\varphi} \sin p\theta \sin\theta \, (1+K\cos\theta) \, [pu_o \, (1+K\cos\theta) + \sin\theta] \, d\theta$

φ deg.	$\frac{b'}{b}$	$\frac{B_2}{u_o(k\delta)}$
37	0.2	u_o (0.2806 − 0.5135 K + 0.2275 K^2) − 0.0570 K + 0.0656
53	.4	u_o (0.6792 − 1.0575 K + 0.4193 K^2) − 0.1528 K + 0.2034
66.5	.6	u_o (1.0284 − 1.4104 K + 0.5095 K^2) − 0.2384 K + 0.3536
79.5	.8	u_o (1.2676 − 1.5548 K + 0.5323 K^2) − 0.2827 K + 0.4673
		$\frac{B_4}{u_o(k\delta)}$
37	0.2	u_o (0.6572 − 1.1842 K + 0.5353 K^2) − 0.0600 K + 0.0678
53	.4	u_o (0.6372 − 1.1842 K + 0.5450 K^2) − 0.0576 K + 0.0608
66.5	.6	u_o (−0.0376 − 0.5216 K + 0.3804 K^2) + 0.0140 K − 0.0858
79.5	.8	u_o (−0.8120 − 0.0614 K + 0.3069 K^2) + 0.0686 K − 0.2702
		$\frac{B_6}{u_o(k\delta)}$
37	0.2	u_o (0.3684 − 0.7347 K + 0.3633 K^2) − 0.0130 K + 0.0131
53	.4	u_o (−0.6792 + 0.7347 K − 0.1545 K^2) + 0.0732 K − 0.1117
66.5	.6	u_o (−0.6900 + 0.8004 K − 0.1848 K^2) + 0.0766 K − 0.1104
79.5	.8	u_o (0.4872 + 0.1290 K − 0.0848 K^2) + 0.0233 K + 0.0771
		$\frac{B_8}{u_o(k\delta)}$
37	0.2	u_o (−0.3593 + 0.5156 K − 0.1738 K^2) + 0.0308 K − 0.0380
53	.4	u_o (−0.2872 + 0.5158 K − 0.2090 K^2) + 0.0264 K − 0.0353
66.5	.6	u_o (0.9296 − 0.7472 K + 0.1218 K^2) − 0.0406 K + 0.1044
79.5	.8	u_o (−0.1272 − 0.2076 K + 0.0508 K^2) − 0.0081 K − 0.0232

λ	1.00			0.75			0.50			0.25		
φ \ A	4	6	8	4	6	8	4	6	8	4	6	8
deg.	$\frac{B_2}{u_o(k\delta)}$											
37	0.1746	0.1380	0.1201	0.1270	0.1017	0.0891	0.0825	0.0673	0.0598	0.0428	0.0361	0.0328
53	.4581	.3725	.3307	.3544	.2913	.2596	.2545	.2120	.1907	.1619	.1374	.1253
66.5	.7393	.6097	.5465	.6002	.4989	.4479	.4647	.3895	.3521	.3368	.2850	.2595
79.5	.9426	.7839	.7050	.7929	.6635	.5969	.6476	.5436	.4917	.5108	.4302	.3905
	$\frac{B_4}{u_o(k\delta)}$											
37	0.3142	0.2314	0.1910	0.2222	0.1657	0.1372	0.1373	0.1041	0.0875	0.0649	0.0509	0.0439
53	.2997	.2195	.1803	.2074	.1537	.1267	.1237	.0924	.0774	.0510	.0398	.0343
66.5	−.0999	−.0952	−.0929	−.1442	−.1235	−.1132	−.1805	−.1465	−.1296	−.2042	−.1610	−.1397
79.5	−.5748	−.4724	−.4225	−.5997	−.4841	−.4262	−.6187	−.4911	−.4273	−.6293	−.4924	−.4240
	$\frac{B_6}{u_o(k\delta)}$											
37	0.1503	0.1038	0.0812	0.0978	0.0681	0.0532	0.0515	0.0362	0.0286	0.0153	0.0110	0.0088
53	−.3664	−.2809	−.2391	−.3101	−.2379	−.2017	−.2503	−.1918	−.1627	−.1858	−.1428	−.1213
66.5	−.3692	−.2823	−.2398	−.3064	−.2347	−.1988	−.2401	−.1840	−.1561	−.1692	−.1302	−.1110
79.5	.2598	.1964	.1684	.3036	.2300	.1932	.3541	.2658	.2214	.4164	.3086	.2555
	$\frac{B_8}{u_o(k\delta)}$											
37	−0.1727	−.1274	−.1054	−.1338	−.0993	−.0819	−.0951	−.0709	−.0588	−.0571	−.0430	−.0360
53	−.1330	−.0968	−.0791	−.0922	−.0677	−.0554	−.0530	−.0393	−.0335	−.0164	−.0127	−.0109
66.5	.4531	.3360	.2788	.4162	.3089	.2552	.3774	.2796	.2307	.3365	.2485	.2052
73.5	−.0709	−.0549	−.0471	−.1006	−.0755	−.0628	−.1365	−.1000	−.0819	−.1819	−.1308	−.1056

TABLE III

Constants for Evaluation of A_n

λ	$A = 4$
1.00	A_2=0.645 B_2+0.099 B_4+0.020 B_6+0.005 B_8 A_4=0.099 B_2+0.295 B_4+0.038 B_6+0.008 B_8 A_6=0.020 B_2+0.038 B_4+0.158 B_6+0.017 B_8 A_8=0.005 B_2+0.008 B_4+0.017 B_6+0.097 B_8
0.75	A_2=0.703 B_2+0.145 B_4+0.030 B_6+0.009 B_8 A_4=0.145 B_2+0.332 B_4+0.086 B_6+0.012 B_8 A_6=0.030 B_2+0.066 B_4+0.179 B_6+0.032 B_8 A_8=0.009 B_2+0.012 B_4+0.032 B_6+0.106 B_8
0.50	A_2=0.810 B_2+0.232 B_4+0.057 B_6+0.016 B_8 A_4=0.232 B_2+0.411 B_4+0.121 B_6+0.024 B_8 A_6=0.057 B_2+0.121 B_4+0.225 B_6+0.061 B_8 A_8=0.016 B_2+0.024 B_4+0.061 B_6+0.122 B_8
0.25	A_2=1.071 B_2+0.456 B_4+0.159 B_6+0.048 B_8 A_4=0.456 B_2+0.639 B_4+0.281 B_6+0.076 B_8 A_6=0.159 B_2+0.281 B_4+0.364 B_6+0.135 B_8 A_8=0.048 B_2+0.076 B_4+0.135 B_6+0.161 B_8
λ	$A = 6$
1.00	A_2=0.972 B_2+0.203 B_4+0.050 B_6+0.014 B_8 A_4=0.203 B_2+0.524 B_4+0.093 B_6+0.022 B_8 A_6=0.050 B_2+0.093 B_4+0.299 B_6+0.043 B_8 A_8=0.014 B_2+0.022 B_4+0.043 B_6+0.188 B_8
0.75	A_2=1.047 B_2+0.272 B_4+0.070 B_6+0.021 B_8 A_4=0.272 B_2+0.586 B_4+0.142 B_6+0.031 B_8 A_6=0.070 B_2+0.142 B_4+0.337 B_6+0.072 B_8 A_8=0.021 B_2+0.031 B_4+0.072 B_6+0.203 B_8
0.50	A_2=1.188 B_2+0.400 B_4+0.119 B_6+0.037 B_8 A_4=0.400 B_2+0.717 B_4+0.238 B_6+0.058 B_8 A_6=0.119 B_2+0.238 B_4+0.421 B_6+0.135 B_8 A_8=0.037 B_2+0.058 B_4+0.135 B_6+0.233 B_8
0.25	A_2=1.500 B_2+0.703 B_4+0.375 B_6+0.090 B_8 A_4=0.703 B_2+1.055 B_4+0.490 B_6+0.146 B_8 A_6=0.375 B_2+0.490 B_4+0.649 B_6+0.250 B_8 A_8=0.090 B_2+0.146 B_4+0.250 B_6+0.300 B_8
λ	$A = 8$
1.00	A_2=1.238 B_2+0.314 B_4+0.087 B_6+0.027 B_8 A_4=0.314 B_2+0.752 B_4+0.164 B_6+0.043 B_8 A_6=0.087 B_2+0.164 B_4+0.451 B_6+0.080 B_8 A_8=0.027 B_2+0.043 B_4+0.080 B_6+0.287 B_8
0.75	A_2=1.333 B_2+0.403 B_4+0.119 B_6+0.038 B_8 A_4=0.403 B_2+0.844 B_4+0.236 B_6+0.060 B_8 A_6=0.119 B_2+0.236 B_4+0.612 B_6+0.123 B_8 A_8=0.038 B_2+0.060 B_4+0.123 B_6+0.313 B_8
0.50	A_2=1.490 B_2+0.560 B_4+0.189 B_6+0.062 B_8 A_4=0.560 B_2+1.016 B_4+0.368 B_6+0.100 B_8 A_6=0.189 B_2+0.368 B_4+0.632 B_6+0.199 B_8 A_8=0.062 B_2+0.100 B_4+ 0.199 B_6+0.355 B_8
0.25	A_2=1.829 B_2+0.916 B_4+0.387 B_6+0.134 B_8 A_4=0.916 B_2+1.439 B_4+0.700 B_6+0.223 B_8 A_6=0.387 B_2+0.700 B_4+0.939 B_6+0.371 B_8 A_8=0.134 B_2+0.223 B_4+0.371 B_6+0.449 B_8

TABLE IV

Values of $\frac{A_n}{u_o(k\delta)}$

λ	$\frac{b'}{b}$	$\frac{A_2}{u_o(k\delta)}$	$\frac{A_4}{u_o(k\delta)}$	$\frac{A_6}{u_o(k\delta)}$	$\frac{A_8}{u_o(k\delta)}$
	$A = 4$				
1.00	0.2	0.146	0.114	0.038	-0.011
	.4	.317	.119	-.040	-.014
	.6	.482	.033	-.040	.041
	.8	.556	-.087	.037	-.002
0.75	0.2	0.123	0.097	0.032	-0.007
	.4	.269	.099	-.034	-.014
	.6	.396	.024	-.033	.038
	.8	.479	-.065	.035	-.001
0.50	0.2	0.100	0.079	0.027	-0.004
	.4	.220	.078	-.030	-.015
	.6	.327	.014	-.026	.035
	.8	.399	-.065	.033	.001
0.25	0.2	0.075	0.061	0.023	0.000
	.4	.166	.053	-.030	-.016
	.6	.257	.001	-.020	.032
	.8	.318	-.066	.031	.004
λ	$A = 6$				
1.00	0.2	0.185	0.158	0.054	-0.013
	.4	.391	.162	-.049	-.020
	.6	.564	.055	-.048	.058
	.8	.674	-.071	.052	-.001
0.75	0.2	0.154	0.131	0.048	-0.008
	.4	.329	.133	-.043	-.020
	.6	.479	.040	-.040	.053
	.8	.576	-.073	.050	.000
0.50	0.2	0.123	0.106	0.039	-0.004
	.4	.265	.103	-.038	-.020
	.6	.393	.023	-.031	.048
	.8	.477	-.077	.047	.002
0.25	0.2	0.089	0.078	0.031	0.001
	.4	.194	.067	-.038	-.021
	.6	.301	.003	-.023	.044
	.8	.372	-.085	.045	.005
λ	$A = 8$				
1.00	0.2	0.213	0.190	0.070	-0.012
	.4	.443	.197	-.058	-.025
	.6	.634	.074	-.054	.072
	.8	.754	-.071	.064	.001
0.75	0.2	0.177	0.159	0.060	-0.008
	.4	.371	.161	-.049	-.025
	.6	.538	.053	-.044	.066
	.8	.648	-.077	.062	.001
0.50	0.2	0.140	0.127	0.050	-0.003
	.4	.295	.122	-.045	-.024
	.6	.437	.031	-.034	.060
	.8	.530	-.085	.059	.003
0.25	0.2	0.099	0.092	0.038	0.001
	.4	.212	.077	-.045	-.026
	.6	.331	.005	-.028	.055
	.8	.411	-.097	.055	.005

TABLE V. Values of Odd Circulation Constants
(Ailerons neutral, $C_L = 1.0$)

λ	A_1	A_3	A_5	A_7
		A = 4		
1.00	0.0796	0.0077	0.0014	0.0004
.75	.0796	.0054	.0019	.0003
.50	.0796	.0022	.0023	.0003
.25	.0796	-.0027	.0024	.0002
		A = 6		
1.00	0.0530	0.0066	0.0014	0.0004
.75	.0530	.0046	.0018	.0003
.50	.0530	.0019	.0021	.0002
.25	.0530	-.0021	.0021	.0002
		A = 8		
1.00	0.0398	0.0058	0.0014	0.0004
.75	.0398	.0040	.0017	.0003
.50	.0398	.0017	.0019	.0002
.25	.0398	-.0018	.0019	.0002

TABLE VI. Additional Lift Factor Due to Aileron Deflection, F_1

Increase of lift on semispan = $2qb^2(k\delta)F_1$

λ	φ deg.	$\frac{b'}{b}$	A		
			4	6	8
1.00	37	0.2	0.028	0.023	0.020
	53	.4	.066	.053	.044
	66.5	.6	.108	.086	.072
	79.5	.8	.148	.119	.100
0.75	37	0.2	0.027	0.022	0.019
	53	.4	.064	.051	.043
	66.5	.6	.106	.085	.070
	79.5	.8	.147	.118	.099
0.50	37	0.2	0.025	0.020	0.017
	53	.4	.061	.048	.040
	66.5	.6	.104	.081	.067
	79.5	.8	.144	.116	.097
0.25	37	0.2	0.023	0.018	0.014
	53	.4	.056	.043	.035
	66.5	.6	.098	.076	.062
	79.5	.8	.141	.111	.093

TABLE VII. Rolling-Moment Factor, F_2
Rolling moment on semispan = $qb^3(k\delta)F_2$

λ	Φ deg.	$\frac{b'}{b}$	A		
			4	6	8
1.00	37	0.2	0.022	0.018	0.016
	53	.4	.047	.038	.033
	66.5	.6	.068	.055	.047
	79.5	.8	.082	.066	.056
0.75	37	0.2	0.021	0.017	0.015
	53	.4	.045	.037	.031
	66.5	.6	.067	.054	.045
	79.5	.8	.081	.065	.054
0.50	37	0.2	0.020	0.016	0.014
	53	.4	.043	.035	.029
	66.5	.6	.064	.051	.043
	79.5	.8	.078	.062	.052
0.25	37	0.2	0.018	0.014	0.012
	53	.4	.039	.030	.025
	66.5	.6	.061	.047	.039
	79.5	.8	.075	.058	.048

TABLE VIII. Additional Induced Drag Factor Due to Aileron Deflection, F_3

When $(k\delta) = 1.0$, induced drag = $\frac{C_L^2 qS}{\pi A}(1+\sigma) + \pi q b^2 F_3$

λ	Φ deg.	$\frac{b'}{b}$	A		
			4	6	8
1.00	37	0.2	0.0146	0.0116	0.0093
	53	.4	.0378	.0266	.0201
	66.5	.6	.0638	.0427	.0312
	79.5	.8	.0906	.0586	.0416
0.75	37	0.2	0.0138	0.0106	0.0085
	53	.4	.0354	.0247	.0182
	66.5	.6	.0614	.0406	.0291
	79.5	.8	.0890	.0574	.0402
0.50	37	0.2	0.0124	0.0094	0.0075
	53	.4	.0320	.0216	.0157
	66.5	.6	.0570	.0371	.0263
	79.5	.8	.0855	.0548	.0383
0.25	37	0.2	0.0106	0.0074	0.0056
	53	.4	.0266	.0168	.0118
	66.5	.6	.0514	.0318	.0223
	79.5	.8	.0810	.0506	.0354

TABLE IX. Ratio of Yawing to Rolling Moment, N/L

λ	φ deg.	$\frac{b'}{b}$	A		
			4	6	8
1.00	37	0.2	0.335	0.248	0.202
	53	.4	.300	.214	.169
	66.5	.6	.281	.200	.153
	79.5	.8	.271	.187	.145
0.75	37	0.2	0.315	0.230	0.186
	53	.4	.282	.198	.155
	66.5	.6	.267	.184	.142
	79.5	.8	.260	.178	.136
0.50	37	0.2	0.286	0.204	0.162
	53	.4	.258	.177	.136
	66.5	.6	.249	.169	.128
	79.5	.8	.246	.166	.126
0.25	37	0.2	0.236	0.161	0.123
	53	.4	.220	.145	.106
	66.5	.6	.223	.147	.109
	79.5	.8	.227	.151	.112

TABLE X. Values of A and B Coefficients for the Roll

λ	A		
	4	6	8
	$\frac{B_2}{u_o\left(\frac{p'b}{2V}\right)}$		
1.00	0.5611	0.4630	0.4139
.75	.4581	.3803	.3412
.50	.3585	.2999	.2709
.25	.2657	.2243	.2036
	$\frac{B_4}{u_o\left(\frac{p'b}{2V}\right)}$		
1.00	-0.0762	-0.0762	-0.0762
.75	-.1311	-.1128	-.1036
.50	-.1796	-.1451	-.1279
.25	-.2182	-.1708	-.1472
	$\frac{B_6}{u_o\left(\frac{p'b}{2V}\right)}$		
1.00	-0.0127	-0.0127	-0.0127
.75	.0119	.0065	.0038
.50	.0421	.0294	.0231
.25	.0808	.0580	.0466
	$\frac{B_8}{u_o\left(\frac{p'b}{2V}\right)}$		
1.00	-0.0046	-0.0046	-0.0046
.75	-.0125	-.0099	-.0085
.50	-.0230	-.0169	-.0138
.25	-.0378	-.0267	-.0212

λ	A		
	4	6	8
	$\frac{A_2}{u_o\left(\frac{p'b}{2V}\right)}$		
1.00	0.3543	0.4339	0.4869
.75	.3033	.3680	.4129
.50	.2505	.3011	.3356
.25	.1964	.2300	.2527
	$\frac{A_4}{u_o\left(\frac{p'b}{2V}\right)}$		
1.00	0.0327	0.0528	0.0702
.75	.0238	.0378	.0505
.50	.0139	.0218	.0288
.25	.0014	.0022	.0027
	$\frac{A_6}{u_o\left(\frac{p'b}{2V}\right)}$		
1.00	0.0064	0.0119	0.0176
.75	.0068	.0120	.0172
.50	.0069	.0115	.0159
.25	.0052	.0089	.0115
	$\frac{A_8}{u_o\left(\frac{p'b}{2V}\right)}$		
1.00	0.0019	0.0034	0.0054
.75	.0016	.0030	.0045
.50	.0014	.0026	.0036
.25	.0010	.0017	.0023

TABLE XI. Factors for the Roll

Additional Lift Factor, F_4

Increase of lift on semispan = $2qb^2 \left(\frac{p'b}{2V}\right) F_4$

λ	A		
	4	6	8
1.00	0.0856	0.0689	0.0579
.75	.0844	.0679	.0566
.50	.0820	.0655	.0547
.25	.0788	.0615	.0508

Damping-Moment Factor, F_5

Damping moment on semispan = $qb^3 \left(\frac{p'b}{2V}\right) F_5$

λ	A		
	4	6	8
1.00	0.0522	0.0425	0.0358
.75	.0511	.0413	.0347
.50	.0492	.0394	.0330
.25	.0463	.0360	.0298

Additional Induced-Drag Factor, F_6

$\left(\frac{p'b}{2V}\right) = 1.0$

Induced drag = $\frac{C_L^2 qS}{\pi A} (1+\sigma) + \pi qb^2 F_6$

λ	A		
	4	6	8
1.00	0.0178	0.0120	0.0085
.75	.0171	.0112	.0079
.50	.0157	.0101	.0071
.25	.0139	.0085	.0058

Ratio of Yawing to Damping Moment, $C_L = 1.0$

λ	A		
	4	6	8
1.00	0.0445	0.0750	0.0920
.75	.0565	.0860	.1020
.50	.0750	.1010	.1160
.25	.1000	.1270	.1390

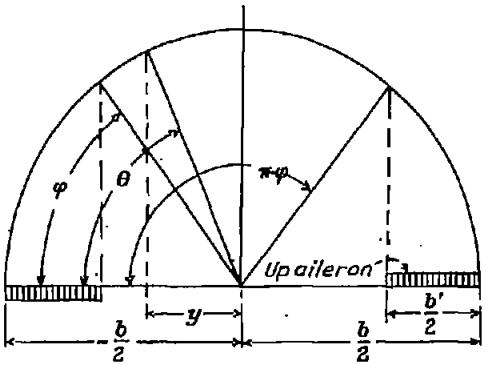

Figure 1.- Definition of angles θ and φ

Wing taper $\lambda = c_t/c_r$	u_0		
	A = 4	A = 6	A = 8
1.00	0.375	0.350	0.188
.75	.429	.386	.314
.50	.500	.333	.250
.25	.600	.400	.300

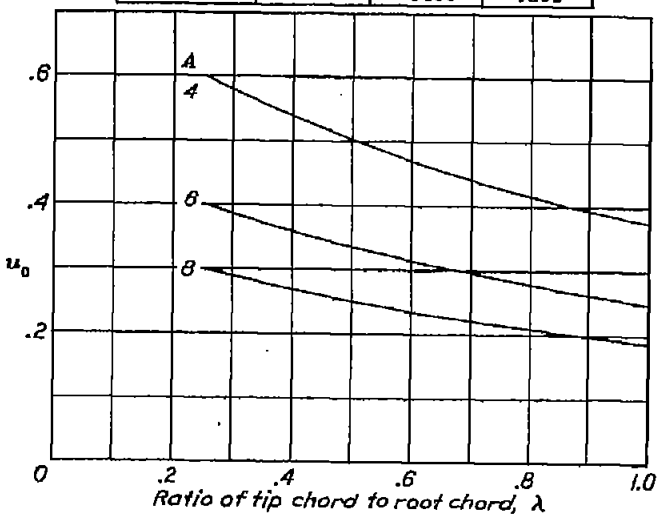

Figure 2.- Variation of u_0 with aspect ratio and taper.

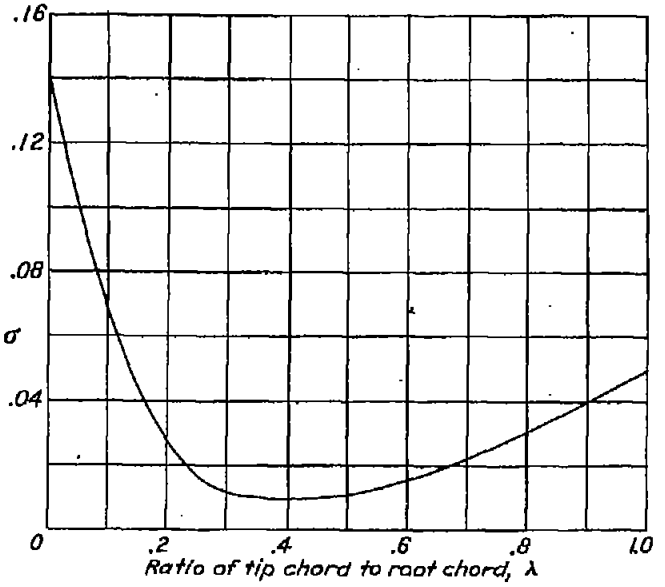

Figure 3.- Theoretical induced-drag factor σ for zero twist, A = 6. (Data from reference 5.)

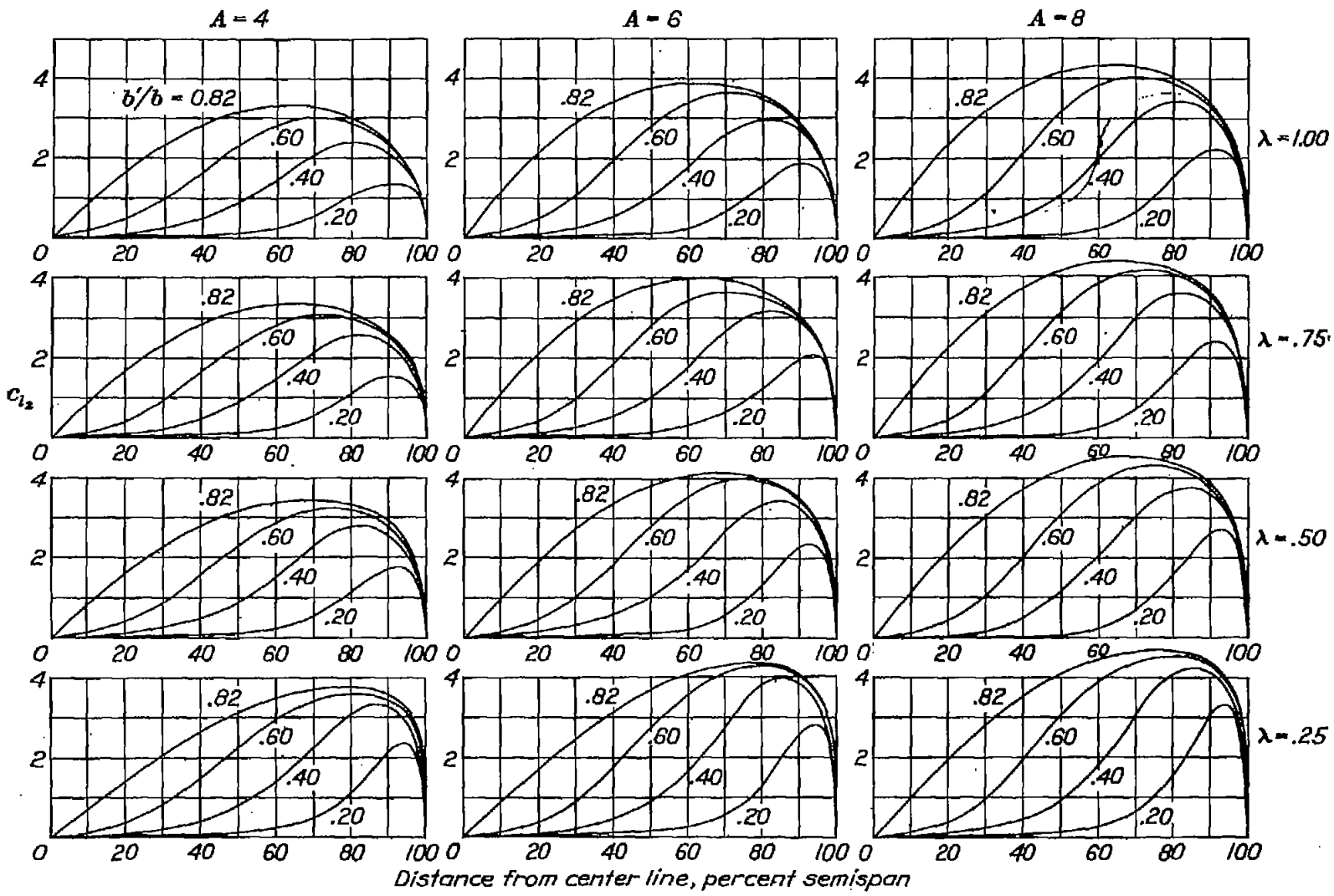

Figure 3.- Theoretical semispan c_{l_2} distribution for (M6) = 1.0.

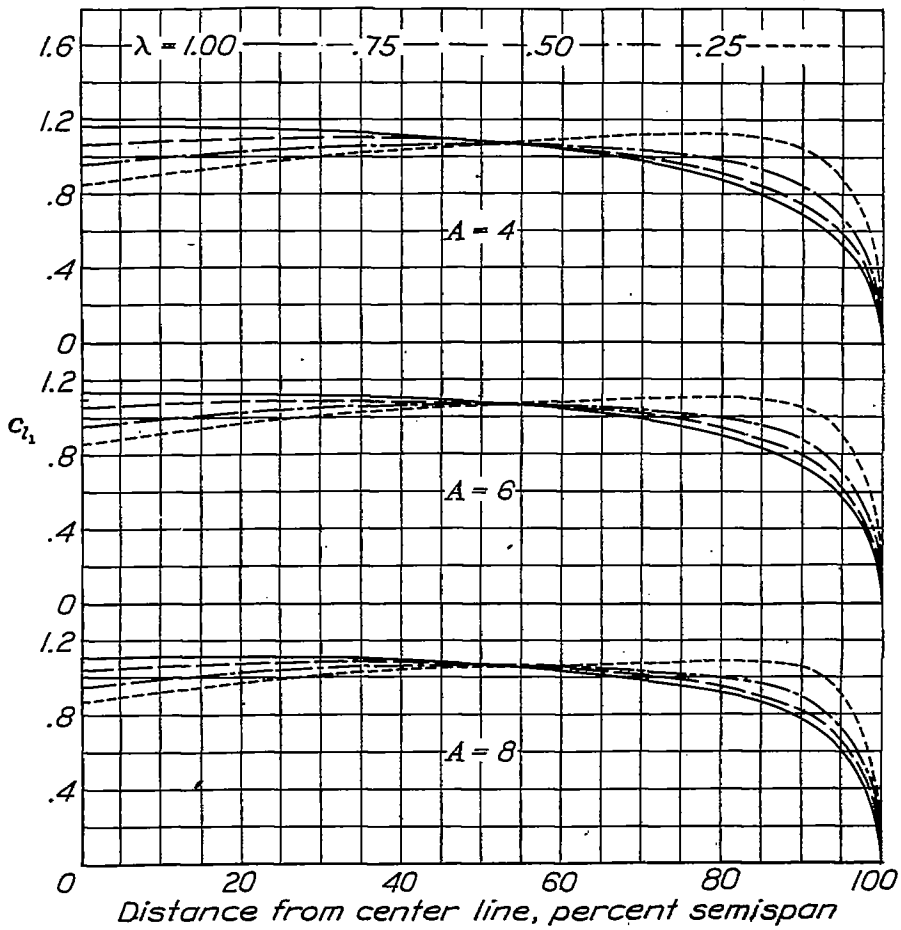

Figure 4.– Theoretical semispan c_{l_1} distribution for wing C_L=1.0

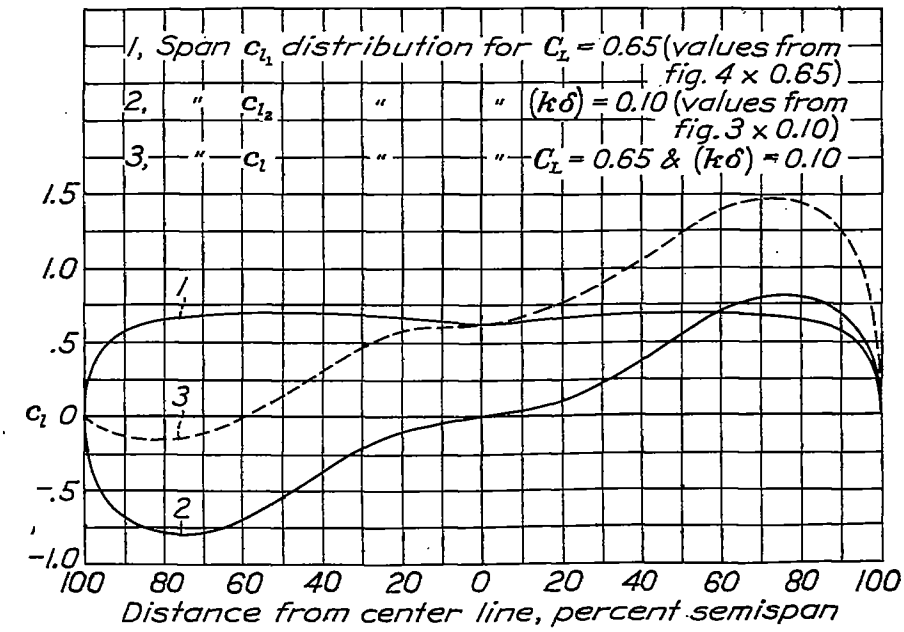

Figure 5.– Theoretical span c_l distribution on tapered wing A=6; λ=0.5; b'/b = 0.6.

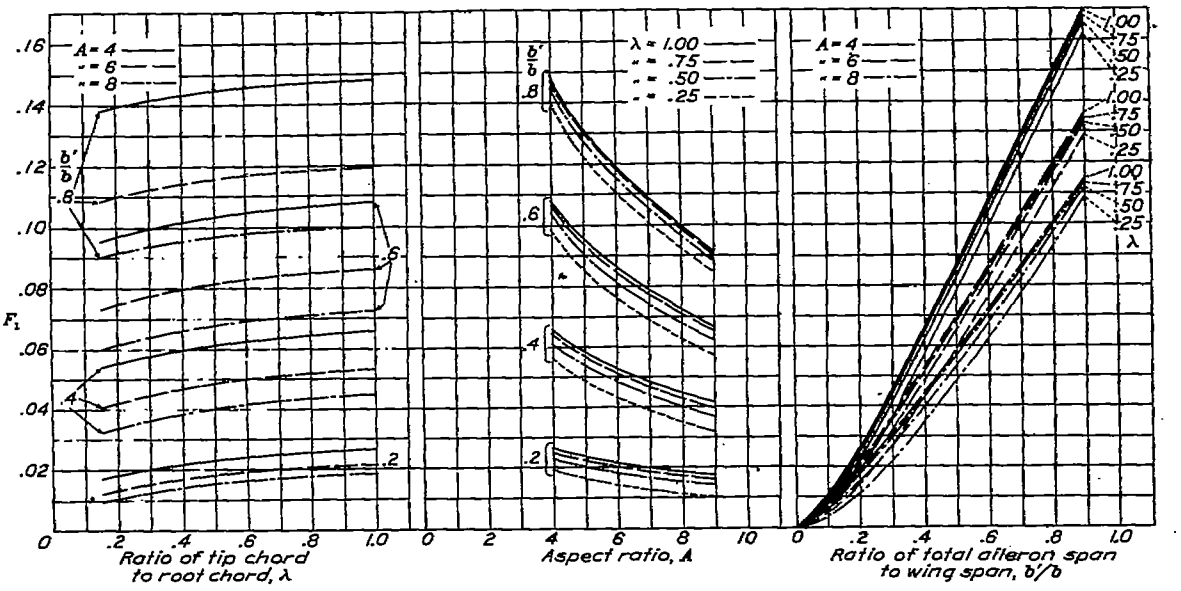

Figure 6.- Theroetical additional-lift factor due to aileron deflection for half the wing, F_1. Additional lift on half the wing = $2qb^2(k\delta)F_1$.

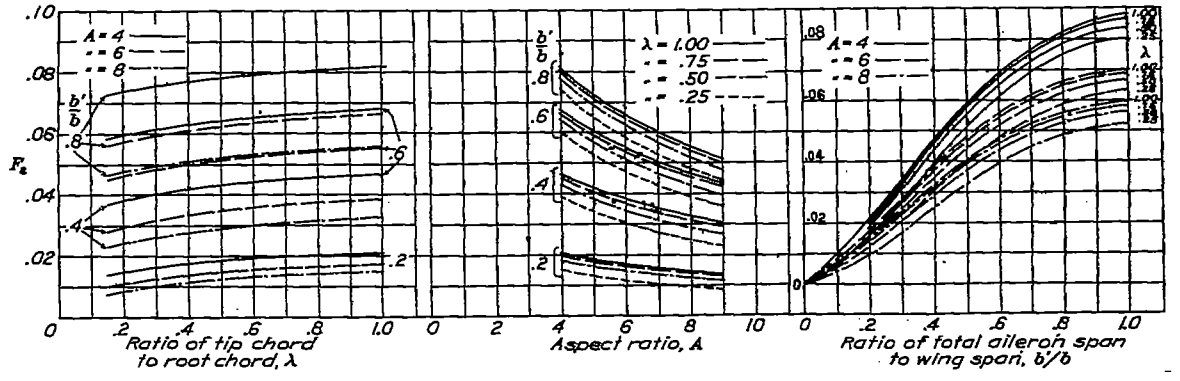

Figure 7.- Theoretical rolling-moment factor, F_2. Total rolling moment= $2qb^3(k\delta)F_2$.

$k = f\left(\frac{\text{aileron chord}}{\text{wing chord}}\right)$

δ: aileron

15 pages

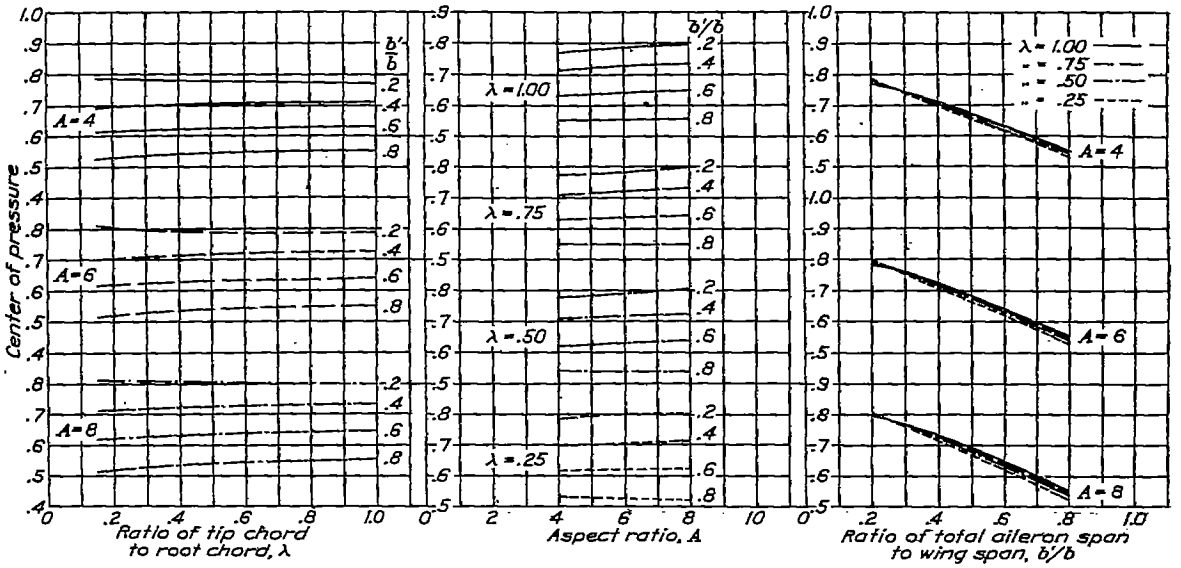

Figure 8.- Theoretical lateral center of pressure of additional load.

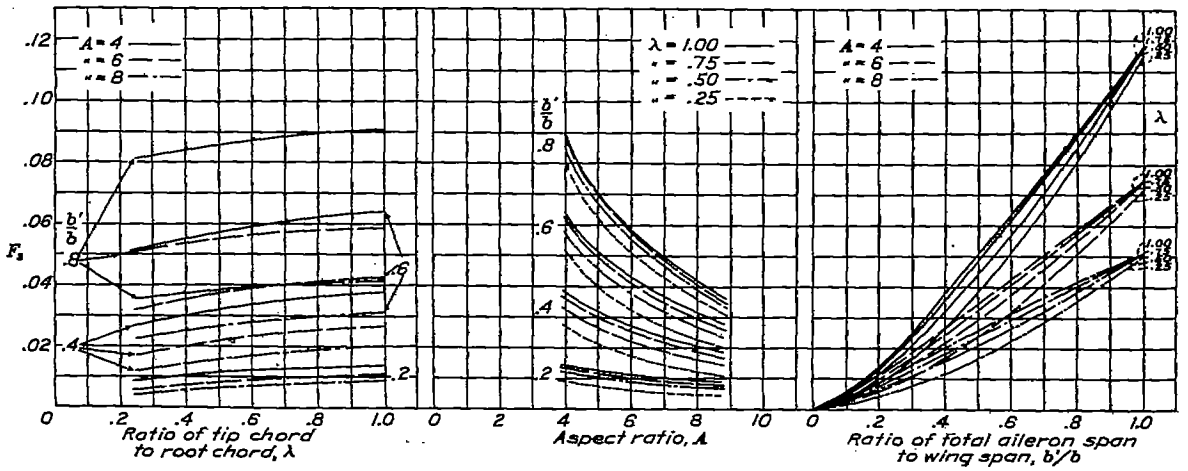

Figure 10.- Theoretical additional-induced-drag factor due to aileron deflection, F_3, for $(k\delta) = 1.0$. Additional induced drag $= \pi q b^2 (k\delta)^2 F_3$.

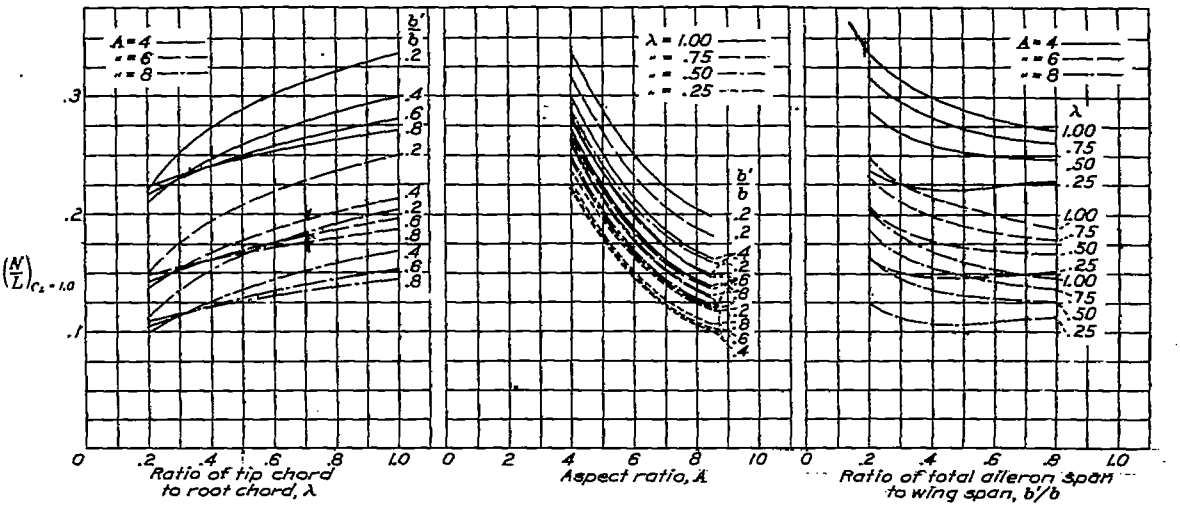

Figure 11.– Ratio of theoretical yawing to rolling moments for $C_L = 1.0$
$N/L = (N/L)_{C_L=1.0} \times C_L$

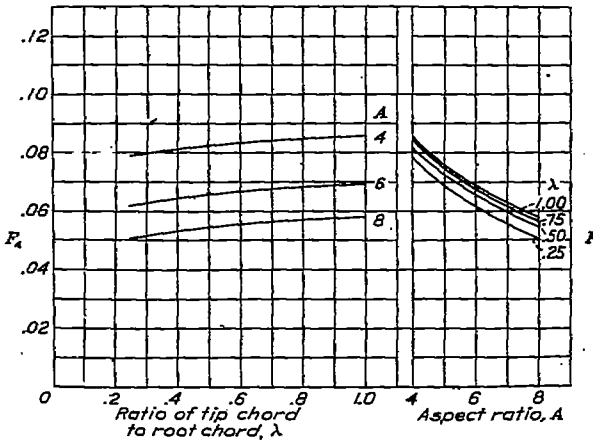

Figure 12.– Theoretical additional-lift factor due to rolling, F4. Additional lift on half the wing $= 2qb^2 (p'b/2V) F_4$.

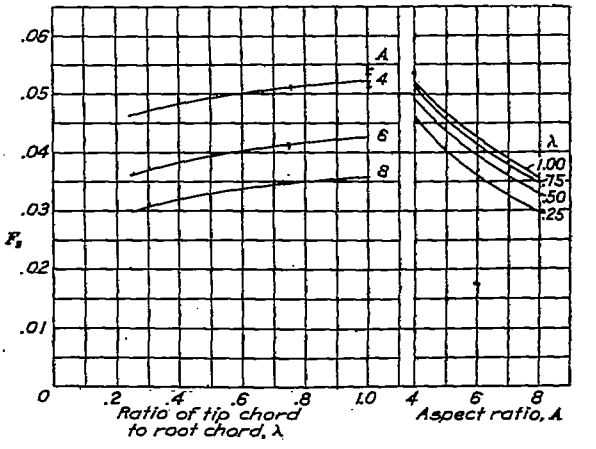

Figure 13.– Theoretical damping-moment factor, F5. Total damping-moment $= 2qb^3 (p'b/2V) F_5$.

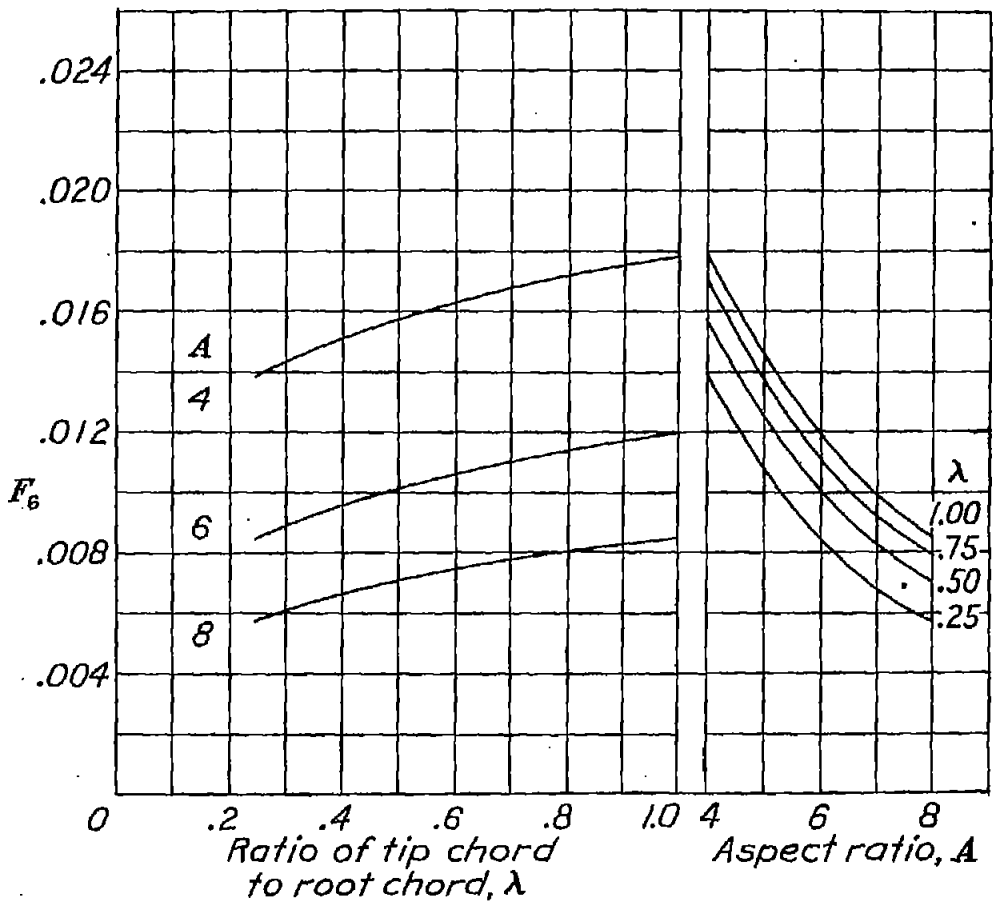

Figure 14.- Theoretical additional-induced-drag factor due to rolling, F_6, for $pb/2V = 1.0$.
Additional induced drag = $\pi q b^2 (pb/2V)^2 F_6$.

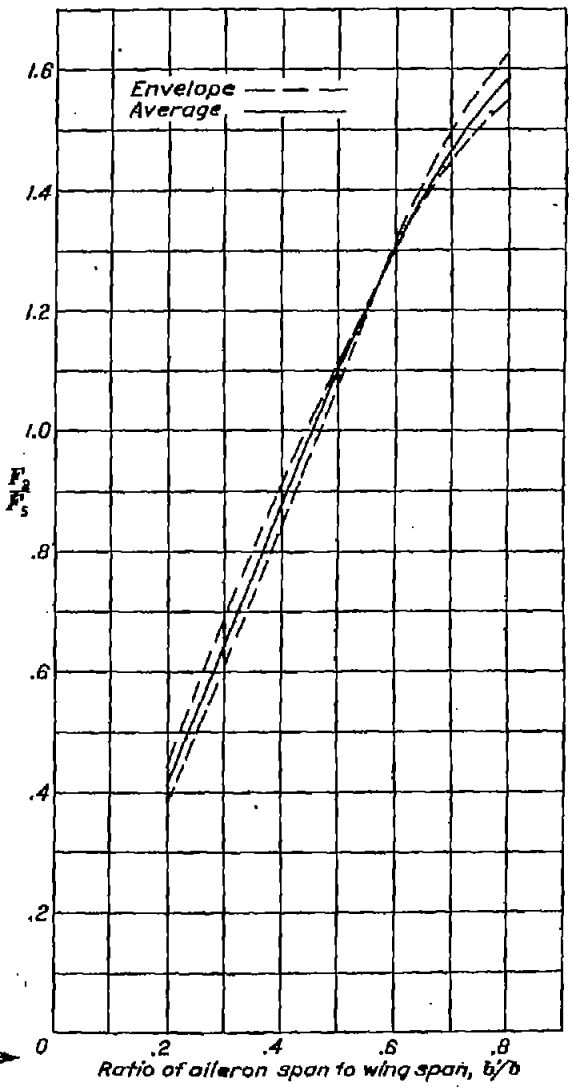

Figure 17.- Theoretically obtainable values of $pb/2V$. $(pb/2V)_{max} = (F_2/F_5)(k\delta)$

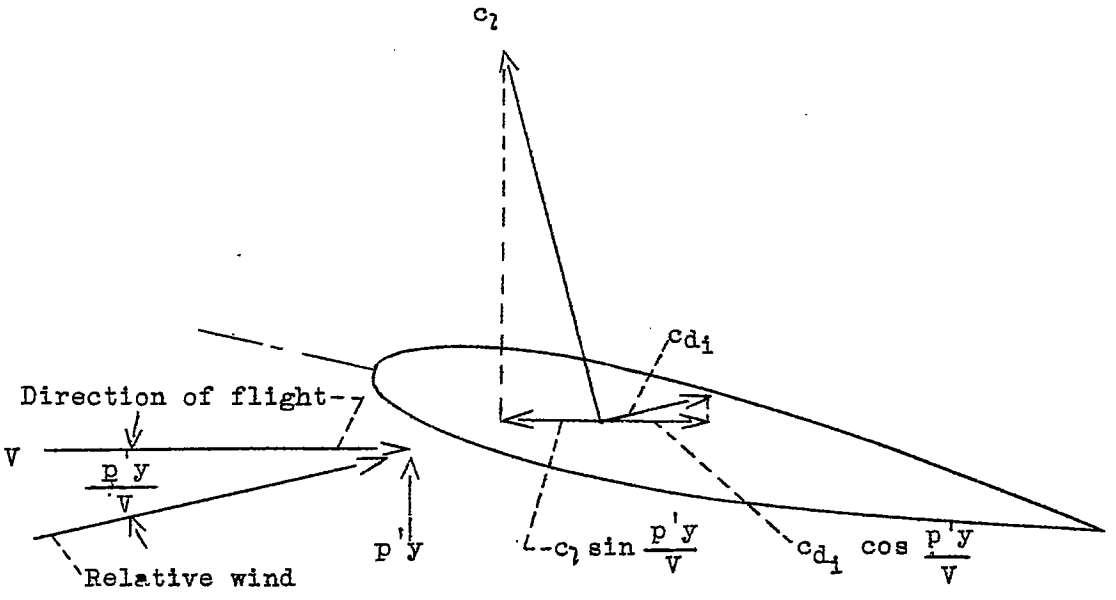

Figure 15.- Yawing components at station y.

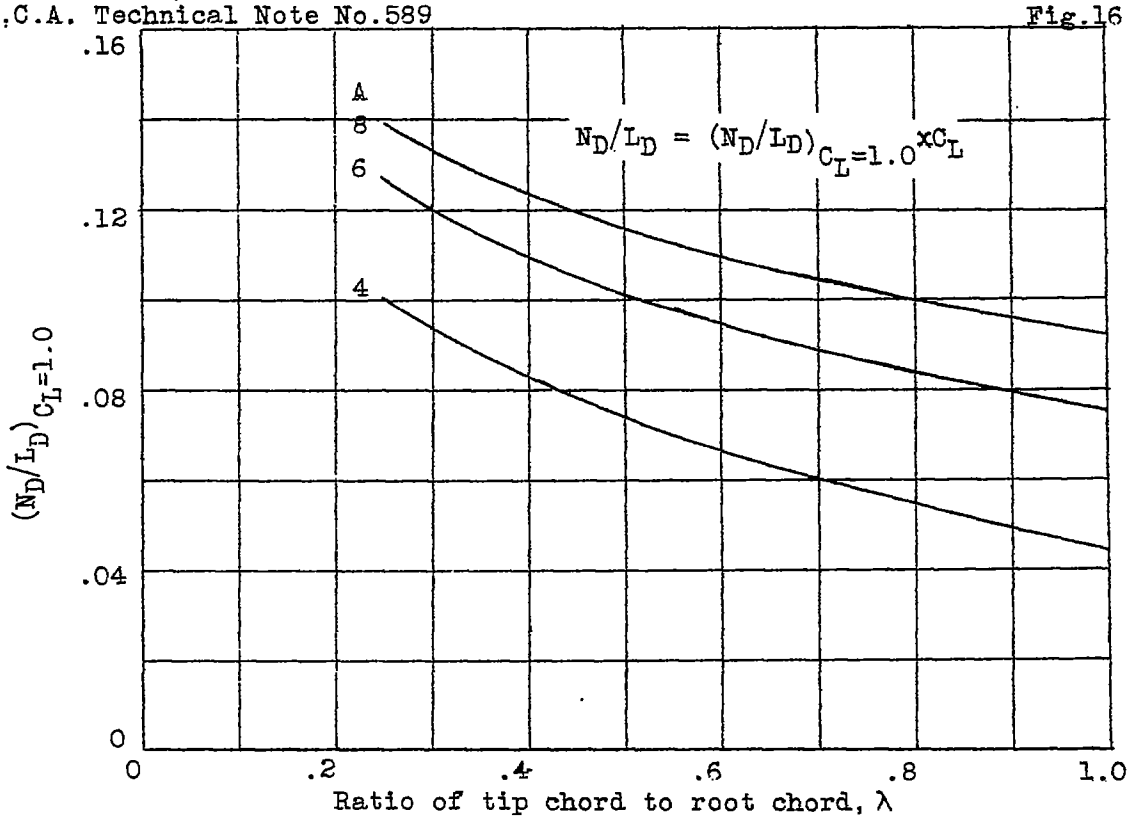

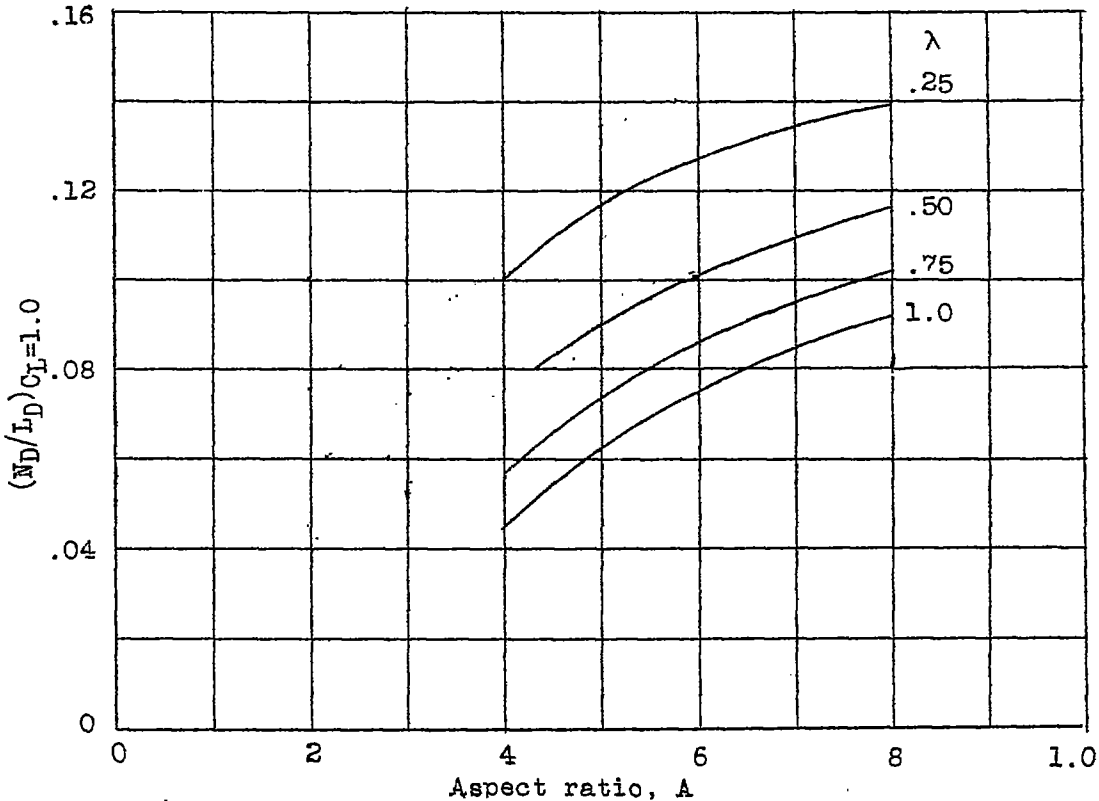

Figure 16.- Ratio of theoretical yawing to damping moments, C_L=1.0.

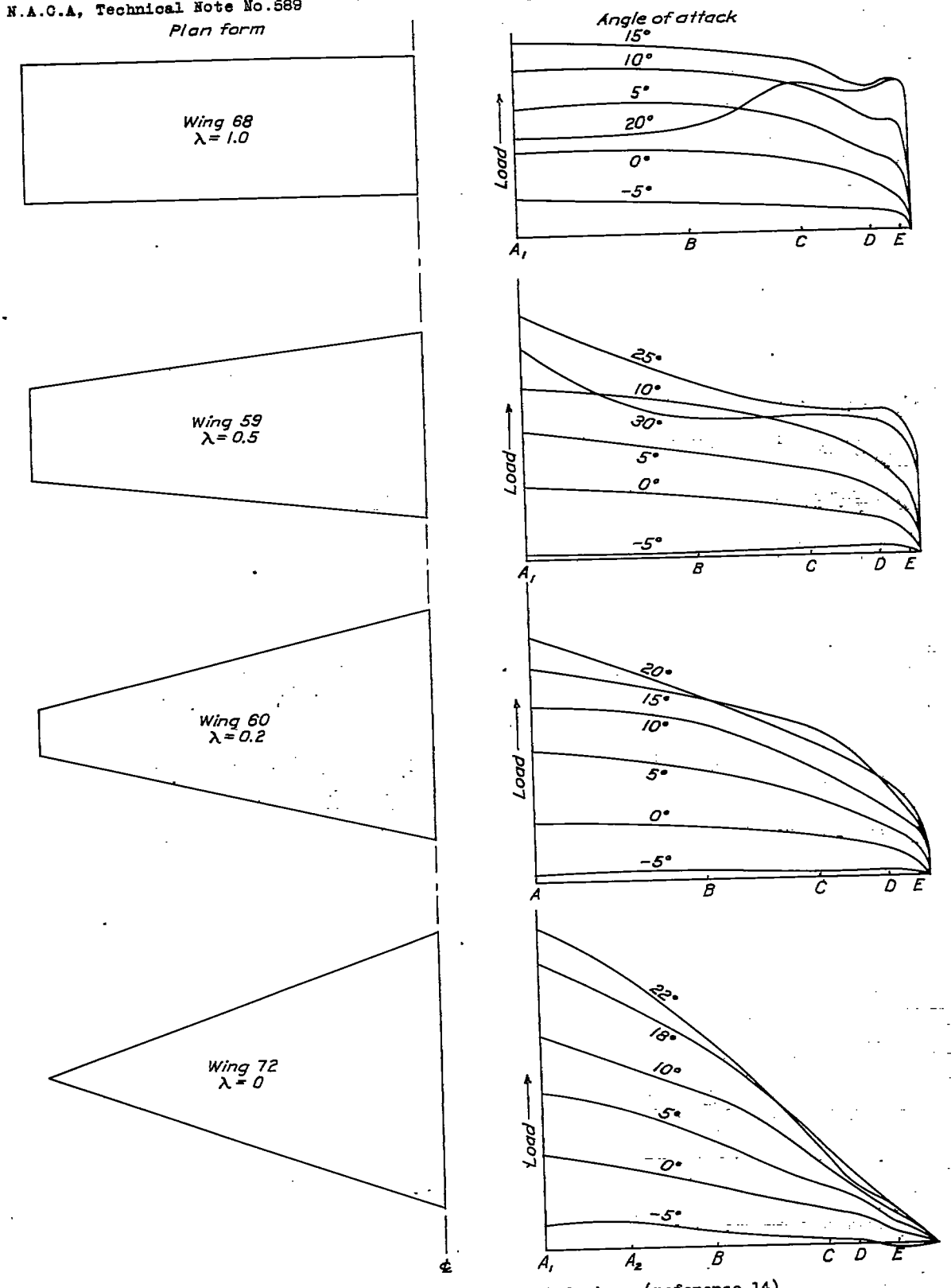

Figure 18.- Span loading for untwisted wings (reference 14)

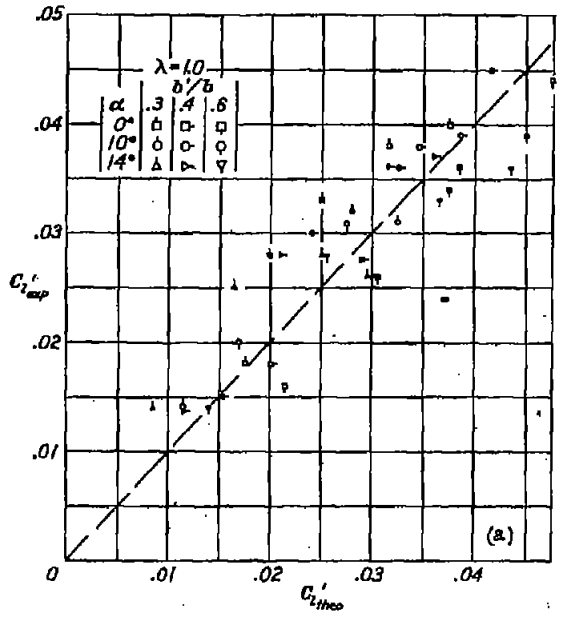

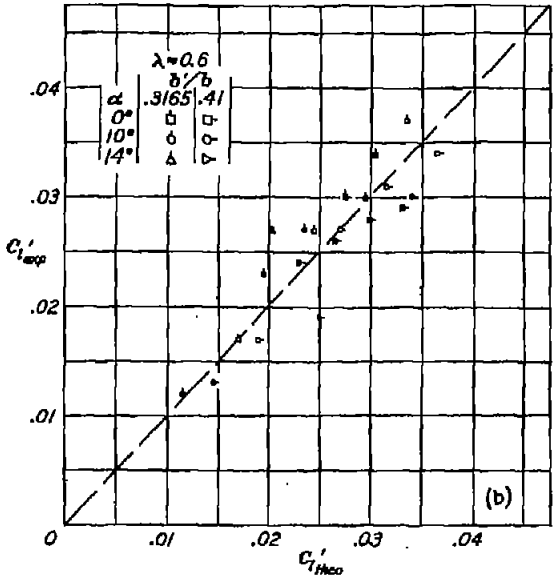

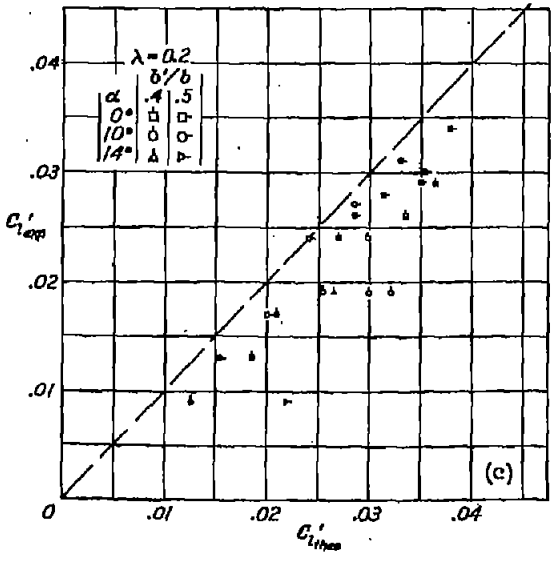

Figure 19 a,b,c.- Comparison of rolling-moment coefficients for three taper ratios.